



WASHINGTON STATE
TRANSPORTATION CENTER

WA-RD 65.3

121 More Hall, FX-10, University of Washington, Seattle, Washington 98195, Telephone: (206) 543-8690



University of
Washington



Washington State
University



Washington State
Department of Transportation

**DEVELOPMENT AND IMPLEMENTATION OF OVERLAY
DESIGN PROCEDURE; INTERIM REPORT NO.2;
ASPHALT CONCRETE STIFFNESS-TEMPERATURE RELATIONSHIP
AND **FILE COPY**
PAVEMENT DISTRESS MODELLING**

by
A. Aziz A. Bubushait
David E. Newcomb
and
Joe P. Mahoney

Prepared by the
University of Washington

for the
Washington State Department
of Transportation

March 1985

1. Report No. WA-RD 65.3	2. Government Accession No.	3. Recipient's Catalog No.	
4. Title and Subtitle Development and Implementation of Overlay Design Procedure, Interim Report No.2: Asphalt Concrete stiffness-Temperature Relationships and Pavement Distress Modeling		5. Report Date March 1985	
7. Author(s) A.A. Bubushait, D.E. Newcomb, and J.P. Mahoney		6. Performing Organization Code	
9. Performing Organization Name and Address University of Washington Department of Civil Engineering Seattle, WA 98195		8. Performing Organization Report No.	
12. Sponsoring Agency Name and Address Washington State Department of Transportation Transportation Building KF-01 Olympia, WA 98504		10. Work Unit No.	
		11. Contract or Grant No. WSDOT Y-2811	
		13. Type of Report and Period Covered	
		14. Sponsoring Agency Code	
15. Supplementary Notes WSDOT Contract Manager - Mr. Art Peters			
16. Abstract This study consists of two parts. The first part discusses the asphalt concrete stiffness-temperature relationship for Class B mix in Washington State. Two relationships have been suggested. The first one is a composite curve for the stiffness-temperature relationship and the other is a correction factor for the stiffness at any temperature. The second part of the report is a state-of-the-art review for the fatigue mode of distress for asphalt concrete pavement.			
17. Key Words Asphalt Concrete Modulus, Stiffness-Temperature Relationship, Distress, Fatigue, and Temperature Correction Factor.		18. Distribution Statement No restrictions. This document is available to the public through the National Technical Information Service, Springfield, VA 22161.	
19. Security Classif. (of this report)	20. Security Classif. (of this page)	21. No. of Pages	22. Price

TABLE OF CONTENTS

LIST OF FIGURES	ii
LIST OF TABLES	iii
INTRODUCTION	1
STIFFNESS - TEMPERATURE RELATIONSHIP	4
Stiffness - Temperature Relationship in the State of Washington.....	5
Summary	20
DISTRESS	21
FATIGUE	23
Fatigue Models	24
Discussion	31
Summary	39
REFERENCES	40
APPENDIX A - The Estimation of Stiffness Modulus of Bituminous Materials by Shell Nomograph	46
APPENDIX B - Methods for Predicting Mean Pavement Temperature	55
APPENDEX C - Regression Analysis	59

LIST OF FIGURES

Number	Page
1. Overall Pavement Overlay Design Strategy.	2
2. Resilient Modulus - Temperature Relationship in Washington State	6
3. Resilient Modulus - Temperature Relationship for AASHTO Road Test	8
4. Resilient Modulus - Temperature Relationship as Developed Using BISDEF Computer Program	10
5. General Stiffness - Temperature Relationship with 90 and 95% Prediction Intervals for Class B Asphalt Concrete in Washington State.	13
6. Data Description for the Stiffness - Temperature Relationship.	14
7. Resilient Modulus Correction Factor	18
8. The Effect of the Value of k_2 on Fatigue Life Prediction	25
9. Fatigue Models	27
10. Relationship between Initial Cracking, 10% Cracking, and 45% Cracking for Finn,etal. Fatigue Model	30
11. Effect of Stiffness Fluctuation on Fatigue life.	32
12. Pavement Life Cycle	35
13. Relationship between Areal Cracking and Damage Index for Finn Fatigue Model	36
14. Nomographic Representation of Distress - Performance Relationship	38
APPENDIX A.	
A.1 McLeod's Chart for Estimating the P.I.	47
A.2 McLeod's Modification of Pfeiffer's and Van Doormal Nomograph	49

LIST OF FIGURES (cont.)

Number	page
A.3	Mc Leod's Modification to Van Der Poel's Nomograph for Determining Asphalt Stiffness 50
A.4	Heukelom's Bitumen Test Data Chart 51
A.5	Standard Penetration - Viscosity Chart 52
A.6	Relationship Between Asphalt Cement Stiffness and Mix Stiffness Based on Heukelom and Klomp Method 54
APPENDIX B.	
B.1	Southgate's Chart for the Prediction of Mean Pavement Temperature 56
APPENDIX C.	
C.1	The Regression Analysis for the Stiftness-Temperature Data 63

LIST OF TABLES

Number	page
1. Stiffness - Temperature Prediction Table.	15
2. Comparison Between the composite M_R -T Chart and the Correction Factor Chart	19
3. Distress and Material Properties	22
4. Numerical Comparison Between Fatigue Models	31
APPENDIX C.	
C1. Stiffness - Temperature Data.	60
C2. A Statistical Summary of the Stiffness - Temperature Data	61

DISCLAIMER

The contents of this report reflect the views of the authors who are responsible for the facts and the accuracy of the data presented herein. the contents do not necessarily reflect the official views or policies of the Washington State Transportation Commission, Department of Transportation or the Federal Highway Administration. This report does not constitute a standard, specification, or regulation.

ASPHALT CONCRETE MODULUS-TEMPERATURE RELATIONSHIPS AND PAVEMENT DISTRESS MODELLING

INTRODUCTION

Generally, pavement failure develops gradually over a span of time. This span of time is defined as pavement life cycle. Most fairly sound pavement sections deteriorate with time in an orderly progress of defects, i.e. as traffic loads, environment, and other factors act upon the pavement system, the pavement responds with stress, strain, deformation and other types of behavior. When this behavior reaches a limiting response value during the pavement life cycle, distress results. The serviceability loss can occur as a result of the accumulation of a single type of distress or a combination of several types (i.e. fatigue cracking, rutting, low temperature cracking, etc.).

Fatigue cracking has been indentified as the predominant type of distress in the United States [13]. Cracks alone do not cause pavement failure. In the case of Washington State, it has been found that there is little or no correlation between the progression of distress and the deterioration of ride. Even though extensive longitudinal or alligator cracking exists, the pavement still rides well. Only when the pavement begins to break up does it demonstrate poor rideability [29].

This report is a satellite study of the Development and Implementation of the overlay design study which is performed jointly by the University of Washington and Washington State Department of Transportation. Figure 1 shows the general concept of the Study. There are two mainfolds to this report. First, to establish a reliable relationship between asphalt concrete

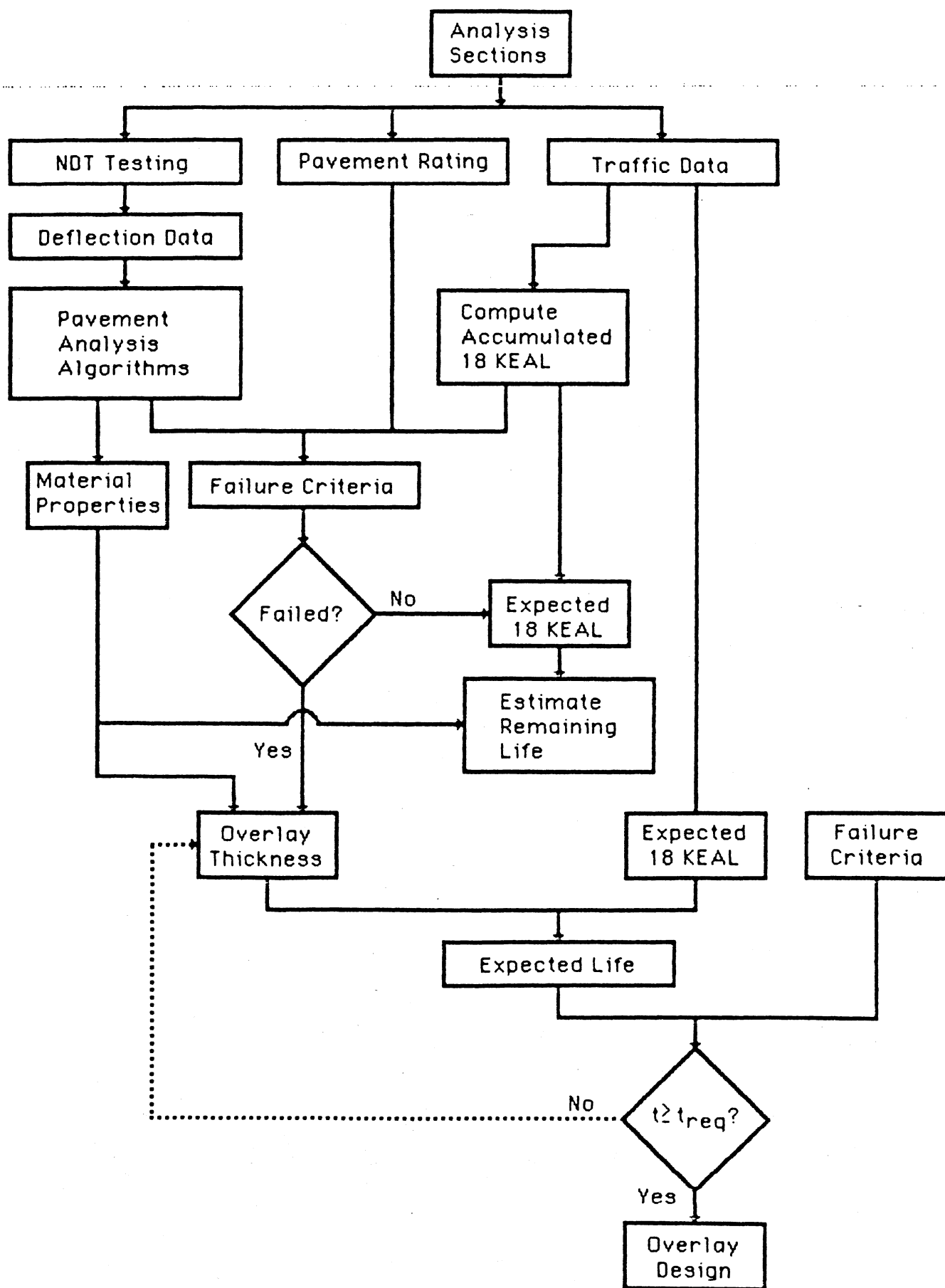


Figure 1. Overall Pavement Overlay Design Strategy.

resilient modulus and pavement temperature. Second, to examine the state-of-the-art in failure criteria and to suggest what is applicable for the State of Washington.

STIFFNESS-TEMPERATURE RELATIONSHIP

Asphalt cement and asphalt concrete mixtures behave as elastic materials at low temperatures and as visco-elastic materials at elevated temperatures. Hence, the stiffness of asphalt concrete is defined as a function of time and temperature [i.e. $S = f(t, T)$]. Both of those factors play a major role in the behavior of asphalt pavement. The importance of asphalt stiffness comes from the fact that all rational pavement design procedures are based on material characteristics such as stiffness and Poisson's ratio. In addition, a literature review reveals that stiffness plays a major role in determining the fatigue and rutting behavior of asphalt concrete pavement.

At short loading times or low temperatures or both, mixture stiffness approaches a constant value and is analogous to a modulus of elasticity. As the time of loading and temperature increase, stiffness decreases. Only the temperature effect will be considered here. In this report, the term stiffness (S), modulus of elasticity (E), and resilient modulus (M_R) are used interchangeably.

A rational method for establishing a relation between temperature and asphalt moduli for the State of Washington is by collecting asphalt concrete specimens from different environmental areas and test them at different temperatures. Since this is not feasible at the present time, the goal in this section is to pool available and reliable information pertinent to the relationship between resilient modulus and temperature in the State of Washington and to compare this with other published criteria.

Stiffness-Temperature Relationship in the State of Washington

Data for the Stiffness-Temperature (S-T) relationship were collected from Washington State University (WSU) test track [1 and 5], Sulphur Extended Asphalt Study [2], the Frost Study [4], the Long Term Monitoring (LTM) sites study [3], the SR 270 highway pavement performance report [40], and the pavement testing for SR 12 report [41].

Figure 2 shows a group of stiffness-temperature curves. The curve labeled (WSU) was obtained from data reported in References 1, 2 and 5 (these references represent the findings of two separate research projects). This curve represents the S-T relationship for cores sampled from the WSU test track in two different studies. It is interesting to note that data from both studies fell in a single stiffness-temperature relationship. This might be due to the fact that both mixes are WSDOT Class B, and the pavement testings were conducted under similar environments.

The group of curves labeled LTM represent the S-T relationship for LTM sites (Sites 1, 3, 5, 6 and 8). Data for the LTM sites were furnished by the Washington State Department of Transportation (WSDOT) and reported in Reference 3. Pavement cores from the LTM sites were tested at only two temperatures (40 and 77°F). Therefore, a group of parallel curves to the WSU test track curves were drawn through the LTM points to extrapolate the relationship.

In general, the S-T relationships for the LTM sites are higher than the WSU test track curve. Many factors can influence the shape of the stiffness-temperature relationship, some of these factors are: 1) the age hardening of the asphalt cement, i.e., asphalt pavement in the LTM Sites has been exposed to

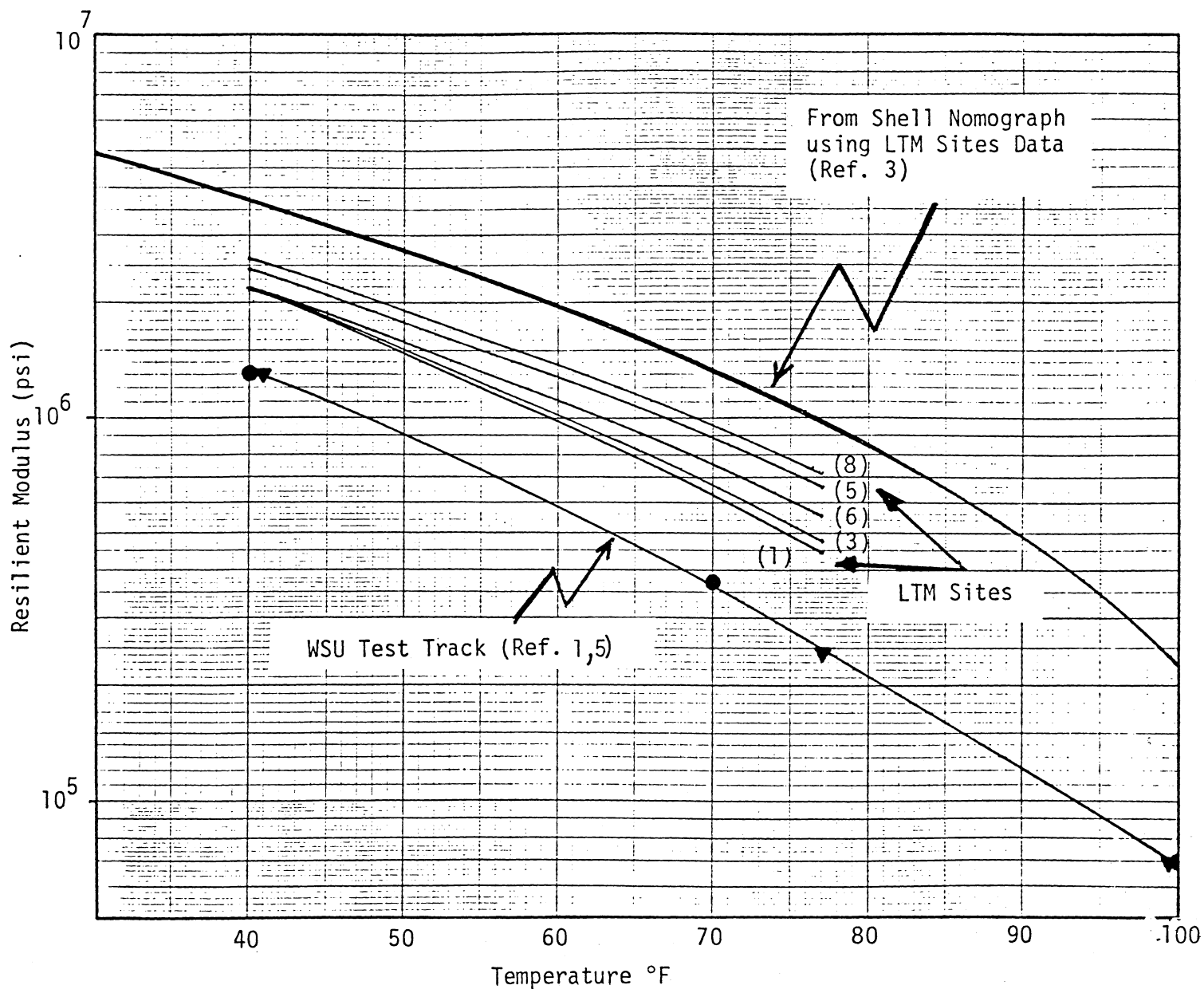


Figure 2. Resilient Modulus - Temperature Relationship in Washington State

the environment for a longer time than the WSU test track asphalt pavement, and 2) the different test equipment used to measure the resilient modulus.

In the LTM study, the material properties were also reported. This can be used to generate more stiffness-temperature points using the Shell nomograph. The Shell nomograph as modified by McLeod [6] was used. To use such a nomograph, viscosity of asphalt cement at 275°F and the Ring-and-Ball temperature are needed. Neither the viscosity at 275°F nor the Ring-and-Ball temperature was reported in Reference 3. Therefore, the viscosity has been estimated from the standard viscosity-penetration chart and the Ring-and-Ball temperature estimated from Heukelom's bitumen test data chart (refer to Appendix A). The intention was to develop a stiffness-temperature curve for each LTM site. But since the viscosity values at 275°F and the Ring-and-Ball temperature were approximated and the accuracy of the nomograph is less than the differences between the S-T relationships for the LTM sites, it was thought that an average curve using the mean values of the LTM material characteristic would give a better representation. The curve developed from the Shell nomograph is also shown in Figure 2. It is obvious that this curve is significantly higher than the laboratory result for the LTM sites. The promising side of this argument is that the curve developed utilizing the Shell nomograph and the LTM sites data can be used to define the slope of the S-T relationship for extreme temperatures in Washington State. It is obvious that the slope of this curve is comparable with both LTM sites and WSU test track curves, especially in the mid-temperature range.

Figure 3 depicts the stiffness-temperature relationship for the AASHO Road Test as reported in Reference 8. Three of these curves represent different test load frequencies (1, 4 and 16 Hz). As loading time decreases (the frequency increases) the resilient modulus increases. The other curve

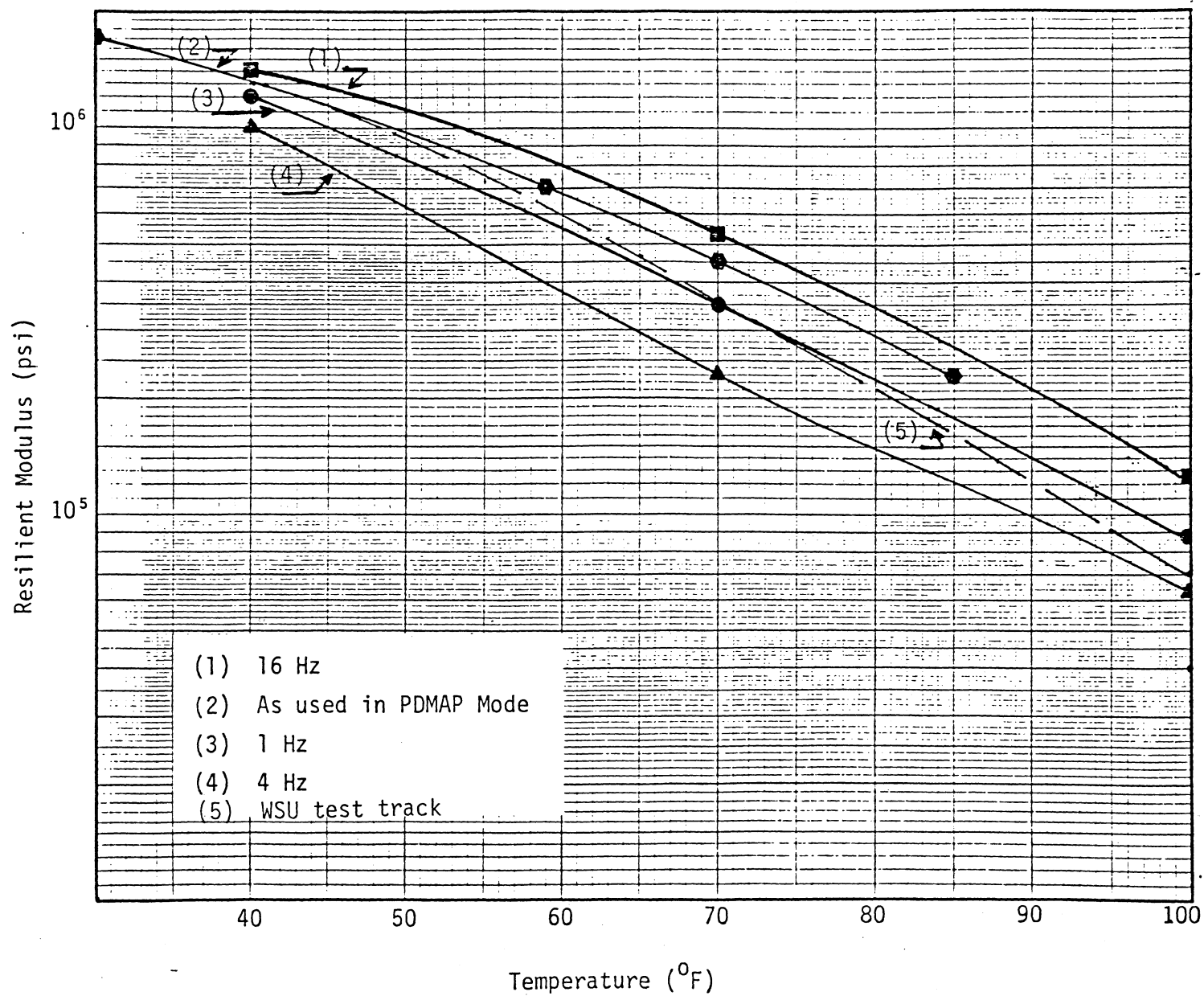


Figure 3. Resilient Modulus - Temperature Relationship for AASHTO Road Test.

represents the relationship of stiffness and temperature as used by Finn and others in developing the distress prediction model (PDMAP).

Comparing the AASHO Road Test results with Washington State relationships reveals a high similarity, especially with the WSU test track results. This is due to the fact that both pavements were new and were subjected to continuous load repetitions until failed. On the other hand, the LTM sites' curves are generally higher than the AASHO curves but have nearly similar slopes. In the comparison analysis, one should bear in mind the different testing equipment used to measure the resilient modulus. But generally speaking, the results of the two studies are very comparable.

Figure 4 shows the S-T relationship for three highway pavements in Chelan County in Washington State. Data for these three highway sections, namely SR 97, SR 2 MP 159.6, and SR 2 Sunnyslope, were reported in the frost study [4]. SR 2 MP 159.6 in fact is a bituminous surface treatment. It should be mentioned here that these data were backcalculated from in-situ deflection measurements.

The BISDEF computer program was used to backcalculate the resilient modulus values. BISDEF is a layered elastic computer program which can be used to determine the resilient moduli of pavement layers and the stresses at any point in the pavement structure from deflection measurements. The resilient moduli as reported in the frost study were associated with surface temperature. Since temperature at the mid-point of the asphalt concrete layer would be a more representative temperature than the surface temperature for correlation purposes, the calculated stiffness-temperature relationships were corrected for the temperature of the mid-point of the asphalt concrete layer. The Southgate procedure, as reported in Reference 9, was used (see Appendix B). The required input for this procedure is the surface tempera-

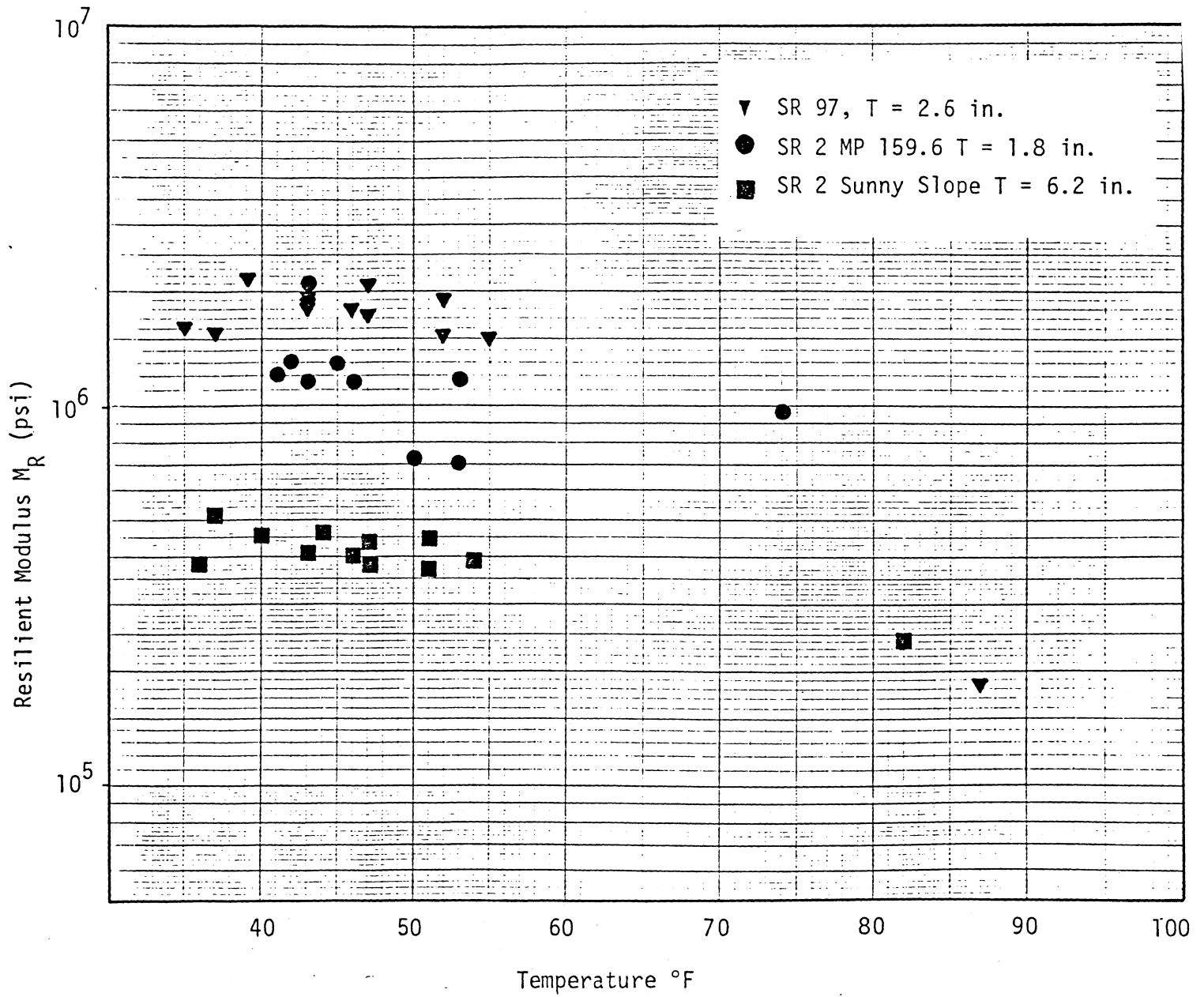


Figure 4.. Resilient Modulus - Temperature Relationship
as Developed Using BISDEF Computer Program.

ture and the previous five day mean air temperature. The latter was obtained from Reference 10.

The frost study data can be divided into two groups as shown in Figure 4. One is for thin asphalt concrete layers and the other for thick asphalt concrete layers. The two highway pavements SR 79 and SR 2 MP 159.6 can be considered as thin asphalt layers since their thicknesses are 2.6 in. and 1.8 in., respectively (SR 2 MP 159.6 is BST). Highway SR 2 Sunnyslope has a thickness of 6.2 in. It is obvious that most of the resilient moduli in the frost study were measured in a narrow temperature range (35-55°F) as shown in Figure 4. Thus, this imposes some limitation on defining the slope of the S-T relationship.

Comparing the results of the frost study with the LTM sites result shows that resilient moduli of highway SR 97 and SR 2 MP 159.6 (thin AC layers) compare very well with the LTM sites moduli. Highway SR 2 Sunnyslope has a significantly lower intercept and flatter slope than the LTM sites. This is attributed to the fact that Highway SR 2 has severe alligator cracking. Such cracks increase the surface deflection measurements which in turn decrease the calculated resilient modulus. In addition, these cracks cause the slope of the relation to become flatter (i.e., less temperature susceptible), since the severely cracked surface acts like a granular material.

In using layered elastic theory and deflection measurements to predict layer elastic moduli (as in BISDEF computer program), some limitations should be considered [3]:

1. The mathematical model for BISDEF computer program (as the case in other layered elastic theory models) does not account for cracking in the pavement section. If a pavement section is in a distressed condition (i.e. cracked) the deflection measurement would be

higher, which results in low BISDEF moduli prediction.

2. A better moduli prediction can be obtained for a thick pavement than a thin pavement section.
3. There is a difference in loading conditions between the field and the laboratory. While asphalt concrete is not particularly stress-sensitive, it does exhibit a small stress-sensitive tendency at high temperatures.

Figure 5 is a general stiffness-temperature relationship for class B asphalt concrete mix in Washington State. Data for this figure were collected from the following studies : the SR 270 highway pavement performance study [40], the SR 12 highway pavement study [41], the LTM sites study and the sulphur extended asphalt laboratory study [43]. Data for these studies were pooled together and modeled using regression analysis. Figure 6 gives a statistical description of the data used in the analysis. Different regression models were tried and the following model gave the best fit according to R-squared and standard deviation:

$$\log M_R = 6.47210 - 0.000147362(T)^2$$

or

$$M_R = 10^{[6.47210 - 0.000147362(T)^2]}$$

where

M_R = asphalt concrete resilient modulus, psi,

T = temperature, °F

In addition, Figure 5 shows the 90 and 95 percent prediction confidencees for the stiffness-temperature relationship. Table 1 presents the resilient modulus, and the 90 and 95 percent prediction intervals for a range of pavement temperatures. This table was calculated from the previous regression model (data and complete analysis is presented in Appendix C).

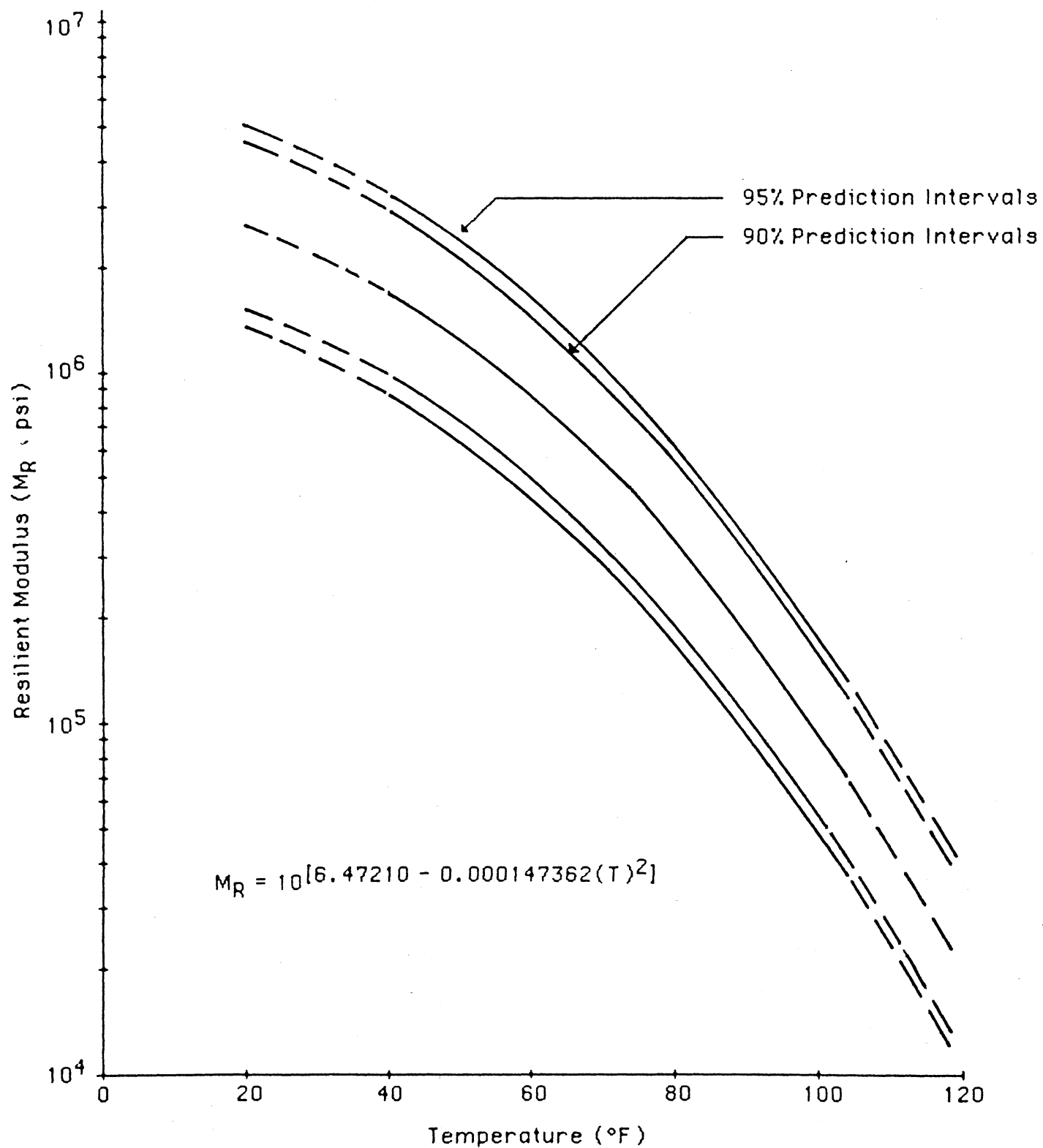


Figure 5. General Stiffness - Temperature Relationship with 90 and 95% Prediction Intervals for Class B Asphalt Concrete in Washington State.

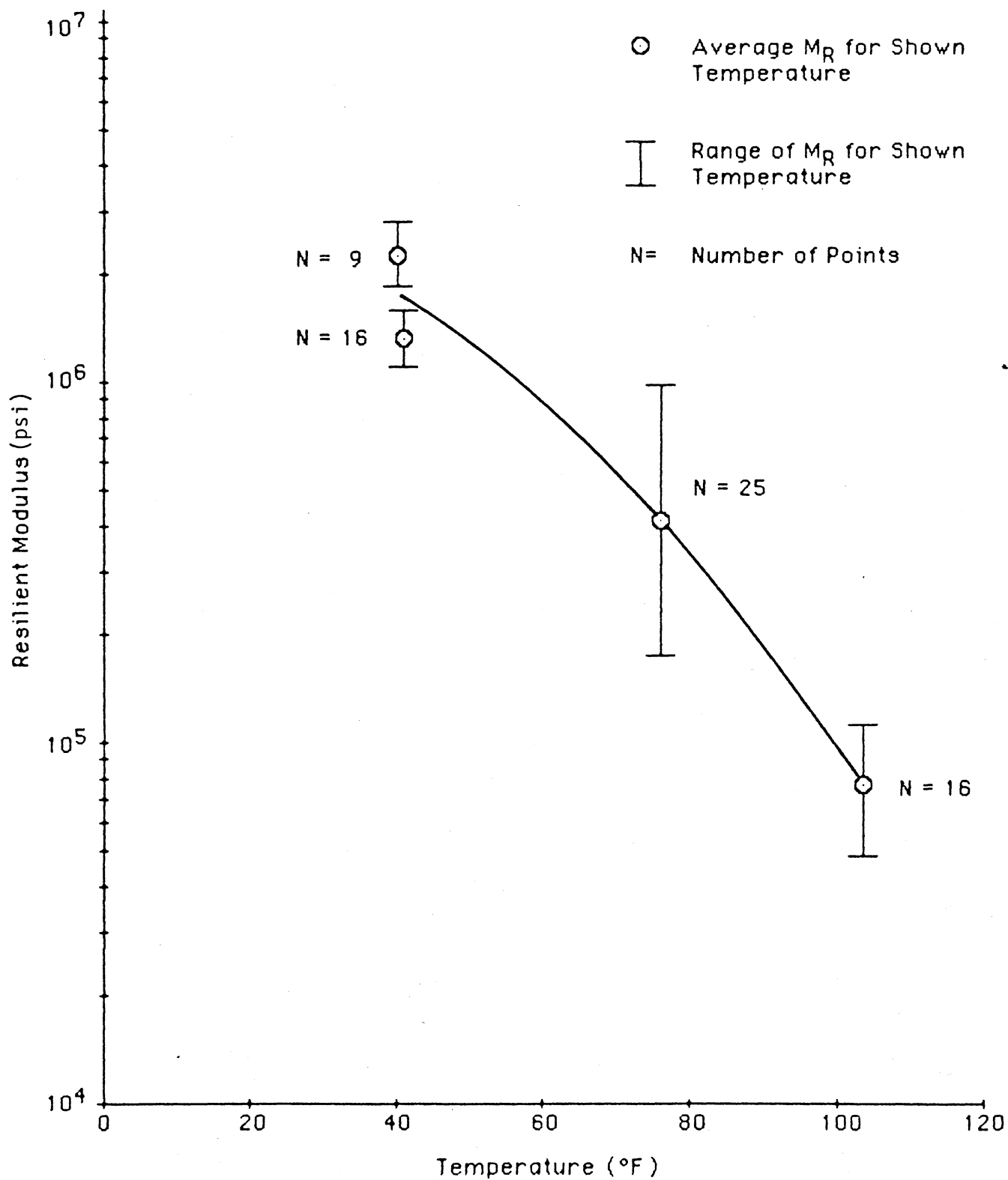


Figure 6. Data Description for the Stiffness - Temperature Relationship.

Table 1. Stiffness-Temperature Prediction Table.

Temp. °F	M _R , psi	95% Prediction Intervals		90% Prediction Intervals	
20.	2589138.	1344797.	4984868.	1496248.	4480297.
21.	2553368.	1326427.	4915226.	1475771.	4417817.
22.	2516383.	1307428.	4843238.	1454595.	4353230.
23.	2478252.	1287835.	4769037.	1432757.	4286655.
24.	2439043.	1267683.	4692759.	1410296.	4218214.
25.	2398826.	1247007.	4614542.	1387253.	4148029.
26.	2357671.	1225843.	4534525.	1363667.	4076226.
27.	2315651.	1204226.	4452850.	1339578.	4002931.
28.	2272836.	1182195.	4369657.	1315028.	3928270.
29.	2229300.	1159785.	4285088.	1290057.	3852371.
30.	2185115.	1137033.	4199287.	1264707.	3775361.
31.	2140352.	1113975.	4112394.	1239018.	3697367.
32.	2095083.	1090650.	4024550.	1213032.	3618516.
33.	2049381.	1067092.	3935896.	1186788.	3538933.
34.	2003316.	1043339.	3846571.	1160328.	3458742.
35.	1956958.	1019425.	3756711.	1133692.	3378066.
36.	1910376.	995387.	3666450.	1106918.	3297026.
37.	1863637.	971258.	3575922.	1080045.	3215740.
38.	1816809.	947074.	3485255.	1053112.	3134325.
39.	1769956.	922867.	3394576.	1026155.	3052893.
40.	1723141.	898670.	3304009.	999212.	2971557.
41.	1676426.	874515.	3213673.	972317.	2890422.
42.	1629872.	850432.	3123684.	945504.	2809594.
43.	1583535.	826452.	3034153.	918807.	2729172.
44.	1537472.	802604.	2945189.	892259.	2649254.
45.	1491736.	778914.	2856896.	865889.	2569932.
46.	1446379.	755410.	2769372.	839728.	2491285.
47.	1401449.	732118.	2682711.	813805.	2413429.
48.	1356994.	709061.	2597003.	788145.	2336414.
49.	1313058.	686263.	2512333.	762775.	2260326.
50.	1269682.	663745.	2428781.	737720.	2185237.
51.	1226906.	641530.	2346422.	713002.	2111214.
52.	1184768.	619635.	2265326.	688642.	2038321.
53.	1143300.	598078.	2185557.	664662.	1966617.
54.	1102535.	576878.	2107176.	641078.	1896154.
55.	1062502.	556049.	2030238.	617910.	1826984.
56.	1023229.	535605.	1954793.	595172.	1759150.
57.	984738.	515560.	1880985.	572879.	1692695.
58.	947053.	495926.	1808556.	551044.	1627653.
59.	910192.	476712.	1737841.	529679.	1564059.
60.	874172.	457928.	1668770.	508793.	1501938.
61.	839008.	439582.	1601370.	488396.	1441317.
62.	804712.	421682.	1535664.	468496.	1382214.
63.	771294.	404232.	1471668.	449098.	1324646.
64.	738763.	387238.	1409396.	430207.	1268624.
65.	707124.	370702.	1348857.	411828.	1214158.
66.	676381.	354628.	1290057.	393963.	1161253.
67.	646535.	339017.	1232998.	376614.	1109910.
68.	617587.	323869.	1177677.	359780.	1060129.
69.	589535.	309185.	1124090.	343463.	1011904.

Table 1. Stiffness-Temperature Prediction Table (Cont.).

Temp. °F	M _R , psi	95% Prediction Intervals		90% Prediction Intervals	
70.	562375.	294962.	1072227.	327659.	965229.
71.	536103.	281198.	1022079.	312367.	920093.
72.	510711.	267891.	973629.	297582.	876484.
73.	486192.	255036.	926860.	283302.	834385.
74.	462536.	242630.	881754.	269520.	793781.
75.	439733.	230666.	838289.	256231.	754651.
76.	417770.	219140.	796439.	243428.	716974.
77.	396635.	208045.	756178.	231105.	680726.
78.	376313.	197374.	717480.	219253.	645882.
79.	356791.	187119.	680313.	207865.	612416.
80.	338052.	177274.	644647.	196931.	580300.
81.	320080.	167829.	610450.	186442.	549505.
82.	302857.	158775.	577687.	176389.	520001.
83.	286367.	150105.	546323.	166762.	491756.
84.	270591.	141809.	516324.	157550.	464739.
85.	255511.	133878.	487653.	148743.	438918.
86.	241107.	126301.	460273.	140330.	414258.
87.	227362.	119069.	434147.	132300.	390727.
88.	214254.	112172.	409237.	124643.	368290.
89.	201765.	105600.	385504.	117346.	346914.
90.	189875.	99342.	362912.	110399.	326565.
91.	178565.	93390.	341421.	103790.	307208.
92.	167814.	87732.	320995.	97509.	288810.
93.	157604.	82358.	301595.	91543.	271336.
94.	147914.	77259.	283184.	85891.	254753.
95.	138726.	72424.	265726.	80513.	239028.
96.	130020.	67843.	249182.	75427.	224127.
97.	121779.	63507.	233518.	70613.	210019.
98.	113982.	59406.	218697.	66059.	196670.
99.	106612.	55530.	204685.	61755.	184051.
100.	99651.	51869.	191448.	57691.	172129.
101.	93081.	48416.	178952.	53855.	160876.
102.	86885.	45159.	167164.	50240.	150261.
103.	81047.	42092.	156053.	46833.	140255.
104.	75550.	39205.	145587.	43627.	130831.
105.	70378.	36490.	135736.	40611.	121962.
106.	65515.	33938.	126471.	37777.	113621.
107.	60947.	31542.	117764.	35115.	105782.
108.	56659.	29294.	109586.	32618.	98420.
109.	52637.	27187.	101911.	30276.	91512.
110.	48867.	25213.	94714.	28083.	85034.
111.	45337.	23366.	87969.	26030.	78964.
112.	42033.	21638.	81652.	24110.	73281.
113.	38943.	20023.	75742.	22315.	67963.
114.	36056.	18516.	70214.	20639.	62990.
115.	33361.	17109.	65049.	19076.	58344.
116.	30846.	15798.	60226.	17618.	54007.
117.	28501.	14577.	55726.	16259.	49960.
118.	26317.	13440.	51529.	14995.	46186.
119.	24283.	12383.	47619.	13819.	42671.
120.	22392.	11401.	43977.	12726.	39398.

To put the results in perspective, the rates of moduli change with temperature were calculated and plotted. Figure 7 shows the rate of change of stiffness with temperature for WSU test track results, AASHTO Road Test results, and the Shell nomograph results. These ratios were calculated by normalizing the resilient moduli with respect to resilient modulus at 77°F. Also shown in the same figure, a relationship developed by Witczak [11], and Hudson and Kennedy [12] for comparison purposes.

Mathematically speaking, the rate of moduli change with temperature can be expressed as $\delta(E_t)/\delta T$. As can be seen, this ratio is a little bit higher in the case of WSU test track results. And it can be assumed equal in the other cases; especially at mid-range temperatures. Regardless, Figure 7 shows a very good comparison between the different studies.

To relate the stiffness-temperature composite curve (Figure 5) with the stiffness-temperature correction curve (Figure 7) Table 2 was developed. Table 2 numerically compares the two methods of predicting the asphalt concrete resilient modulus for a range of temperature. The resilient modulus at 77°F from Table 1 was chosen to be the base value ($M_R = 396,635$ psi). This value then corrected for other temperatures using the correction factor from Figure 7. Table 2 shows a very good agreement between the two methods.

In conclusion, Figures 5 and 7 are very useful charts for examining the effect of temperature on resilient modulus in Washington State. Figure 5 could predict the asphalt concrete resilient modulus with no previous information. In addition, Figure 7 (curve 4 in Figure 7) which is developed using the LTM sites data and utilizing the Shell nomograph can be used to define the resilient modulus-temperature relationship if only one point is known.

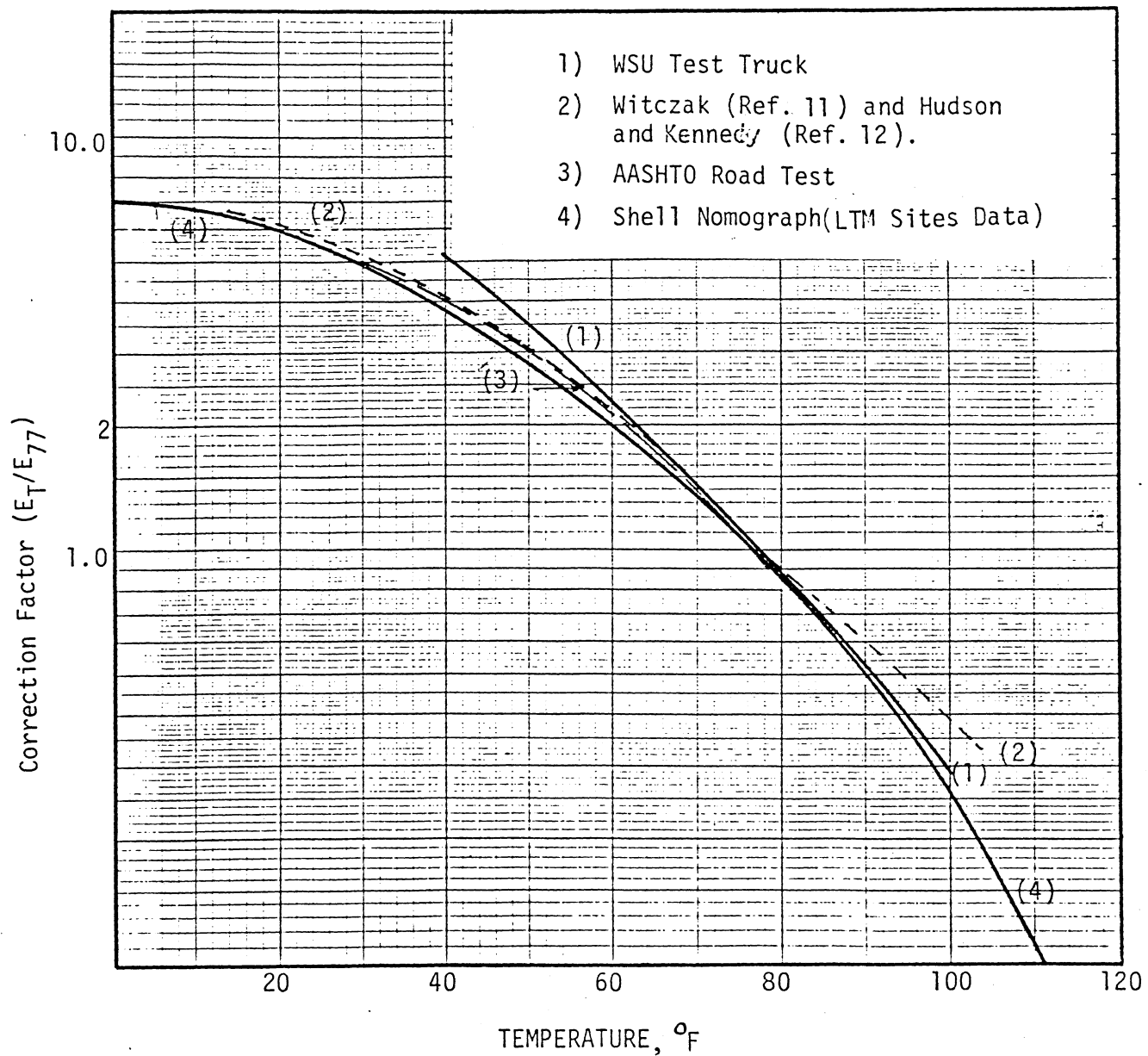


Figure 7. Resilient Modulus Correction Factor.

Table 2. Comparison Between the Composite M_R -T Chart and the Correction Factor Chart.

Temp. °F	Correc- tion Factor From Fig 6.	M_r Corrected (A)	M_r from Figure 5 (B)	Percentage Difference $= \frac{A-B}{B} \times 100$
20.	6.00000	2379610.	2589138.	-8.0849
30.	4.80000	1903848.	2185115.	-12.8720
40.	3.80000	1507213.	1723141.	-12.5311
50.	2.80000	1110578.	1269662.	-12.5310
60.	2.00000	793270.	874172.	-9.2547
70.	1.35000	535457.	562375.	-4.7864
80.	.85000	337140.	338052.	-.2699
90.	.50000	198318.	189675.	4.4453
100.	.25500	101142.	99651.	1.4961

Reasons behind recommending curve 4 (in Figure 7) include:

1. It is more conservative at high and low temperatures,
2. It is equal to other models in mid-range temperature, and
3. It was developed based on Washington State material characteristics.

Summary

The stiffness-temperature relationship is an important element of pavement design. There are at least three procedures to establish such relationships: 1) a direct procedure or laboratory testing, 2) indirect procedures such as backcalculating the resilient modulus from in-situ deflection measurements, and 3) the Shell nomograph.

The recommended correction factor nomograph was developed using the LTM sites and the Shell nomograph. This nomograph was compared with other documented models and gave almost identical results.

DISTRESS

Generally, there are three principle distress modes in flexible pavements. Two of these are traffic associated distress and the third mode is environmental associated distress. Namely, these distress modes are: fatigue cracking, permanent deformation (rutting) and low temperature cracking.

Fatigue in asphalt pavement is caused by the repetitive application of traffic loads which induce stresses and strains sufficient to cause damage and thus loss of serviceability. Usually fatigue cracking is initiated in the lower fiber of the asphalt concrete layer due to the accumulation of tensile strain and extended through the asphalt blanket.

Permanent deformation or rutting is the result of cumulative permanent deformation or plastic flow in one or more of the constituent layers of the pavement. The surface deformations are caused by a combination of densification (a decrease in volume) and shear deformation (plastic flow with no volume change). Rutting appears as a longitudinal depression in the wheel path area due to intensive load applications [20].

Low temperature or transverse cracking is caused when tensile stresses induced by frictional resistance of the underlying layer to thermal contraction of the surface layer exceeds the tensile strength of the surface material [14].

Table 3 summarizes the material properties that have a great influence on the distress type. Since fatigue cracking is the main form of distress in Washington State and the Washington State Department of Transportation Pavement Management System (WSDOT PMS) uses cracking as the primary criteria in indentifying pavement distress, the discussion here will be limited to fatigue distress. Other types of distress are discussed elsewhere [8, 14, 15, 16, 17, 18, 19].

Table 3. Distress and Material Properties.

MATERIAL PROPERTIES	DISTRESS TYPE		
	Fatigue Cracking	Rutting	Low-Temperature Cracking
	1) M_R of AC LAYER 2) M_R of Base Materials 3) ϵ_t of AC 4) Void Content	1) M_R of AC LAYER 2) M_R of Subgrade Soil 3) Permanent Deformation for AC Surface 4) Permanent Deformation for Subgrade Soil	1) Coefficient of Thermal Expansion for AC 2) Stiffness Modulus for AC 3) ϵ_t of AC

Fatigue

There are several different design procedures available to consider fatigue distress. Generally speaking, these procedures range from laboratory developed criteria to criteria developed primarily from performance studies of existing pavements. Some procedures are indentified as "phenomenological" which, in essence, form an empirical relationship between an applied stress or strain level to observed repetitions to fracture or failure. Others are called "mechanistic" which are based upon continuum fracture mechanics.

There are two schools of thought in the assessment of the state-of-the-art of fatigue distress. Both of these are design oriented. One is the "safe fatigue design procedure", and the other is the "prediction of pavement systems future performance" [28]. Since the former is a simple and easy procedure to employ, most of the available literature deals with this type of design. The latter procedure might be described as the ultimate design procedure. In order to specify a procedure that can predict future pavement performance, the interaction of initial fracture, rate of crack propagation, subsequent distress-to-performance relationships, and a failure level based on functional concepts all should be considered in a complete fatigue subsystem.

In the phenomenological procedure, it has been found that the tensile strain at the bottom of an asphalt layer is a good determinate of damage induced by traffic load repetitions. Furthermore, some researchers [8, 38] found that adding a stiffness term to the fatigue equation gives a better correlation. The advantage of such a term is that it makes the model more sensitive for the asphalt concrete temperature; but does not identify the variations in the strain value itself. Usually Miner's summation is used to

account for the strain variation [39]. The general relationship used to represent the fatigue response is of the form:

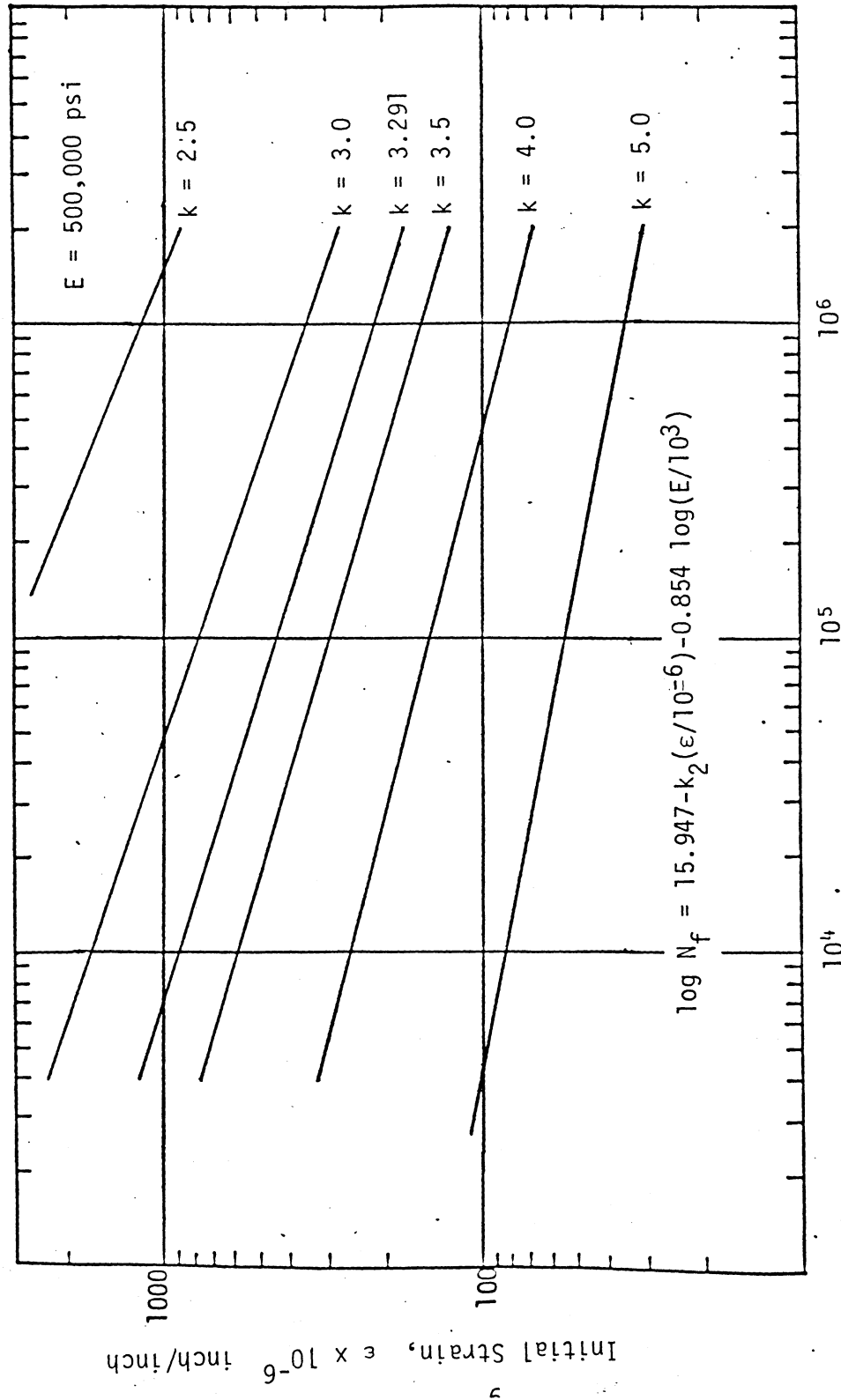
$$N_f = k_1 (1/\epsilon_t)^{k_1} (1/E)^{k_2}$$

where N_f is the number of repetition or application to failure, ϵ_t is the repeatedly induced tensile strain, E is the asphalt concrete resilient modulus, and k_1 , k_2 and k_3 are fatigue parameters or regression constants. A summary of fatigue parameters k_1 and k_2 as reported for a variety of design mix conditions are presented in Reference 20. For conventional asphalt mixtures values of k_1 generally range from 10^{-20} to 10^{-5} while values of k_2 range from 2.5 to 6.5 [21]. Some researchers have demonstrated that the two fatigue parameters are not independent of each other and there is a very strong correlation between them.

The fatigue model is most affected by the value of k_2 , since it is an exponential term. A low k_2 value produces a steep fatigue line and a high k_2 value produces a flat fatigue line as shown in Figure 8. This chart was developed by holding all variables constant and varying the value of k_2 in the Finn, et al. model [8] (assuming no correlation between k_1 and k_2). This figure indicates that values of k_2 below 3 produced a steep fatigue line and values above 4 produced flat curve compared with the models in the literature.

Fatigue Models

The fatigue relationship has received a tremendous amount of research in the past 20 years. Most of the reported research has dealt with identifying the effects of design mix variables on fatigue performance or the development of a prediction model for design purposes. Most of the fatigue studies have been based on laboratory testing, with very little attempt to correlate results with pavement performance. Thus, there is a considerable



Applications to Failure, N_f

Figure 8. The Effect of the Value of k_2 on Fatigue Life Prediction.

amount of literature to determine fatigue cracking, but very little knowledge regarding the prediction and progression of cracking in actual pavements.

Representative fatigue curves are shown in Figure 9. These curves were reported by Pell and Brown [22, 23], Monismith, et al. [24], Kingham [25], Austin Research Engineers (ARE) [26], Majidzadeh [30], and Finn, et al. [8].

Pell and Brown [22, 23] have performed extensive laboratory fatigue studies. Most of the work has been concentrated in the constant stress mode. From their studies, they concluded that the most important mix variables affecting the fatigue life were the binder content and degree of mix compaction. Various shift factors ranging from 20 to 100 have been suggested by Pell and Brown. The Pell and Brown model in Figure 9 represents a laboratory fatigue curve adjusted to field conditions (a shift factor of 20 was used).

Monismith and others have conducted extensive laboratory studies relative to the effects of mix properties upon fatigue behavior of bituminous mixes. It has been found that the two most influential parameters affecting the fatigue life were the mix stiffness and air void content. The mix stiffness was found primarily to affect the slope of the fatigue relationship. Mixes with higher stiffness have flatter slopes than mixes with lower stiffnesses.

Kingham has developed a fatigue criteria based upon an extensive multi-layered elastic analysis of the AASHO Road Test. Kingham found that the fatigue relationship is influenced by the test temperature. In addition, it has been found that there is a unique strain-life relationship for each test temperature. The final fatigue model as developed based on a terminal serviceability level of $P = 2.5$, is:

$$\log \epsilon = 1.2458 - 0.67296 \log E - 0.0065461 \log N_f - 0.034001 \log E \log N_f$$

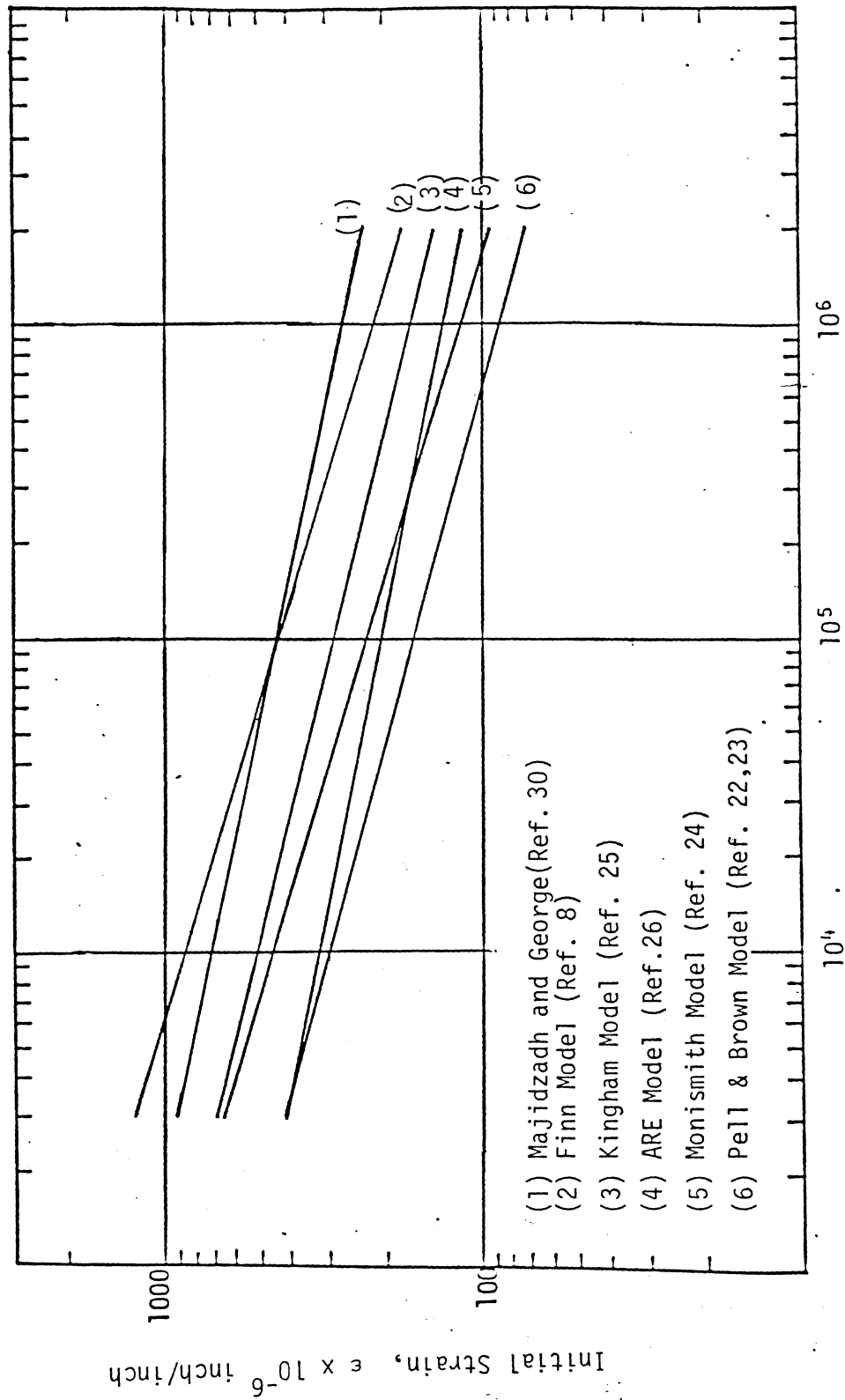


Figure 9. Fatigue Models

where :

ϵ = asphalt concrete tensile strain,

E = asphalt concrete resilient modulus,

N_f = number of load applications until failure.

The fatigue criteria developed by Austin Research Engineers (ARE) is also based on data from the AASHO Road Test. Twenty-seven sections which included traffic repetitions and predicted tensile strains were analyzed. The final fatigue model is as follows:

$$N_f = 9.7255 \times 10^{-15} [\epsilon]^{5.16267}$$

where N_f is the number of weighted 18-kip axle loads prior to Class 2 cracking. The distress model developed by Majidzadeh and others [30] for the FHWA-RII overlay design procedure is also based on AASHO Road Test data. Contrary to the FHWA-ARE model, the stress dependency of the subbase and subgrade layer were consider in developing this model. The final fatigue model is:

$$N_f = 7.56 \times 10^{-12} (\epsilon)^{4.68}$$

Although both the FHWA-ARE and the FHWA-RII fatigue models were derived from the same distress data, Majidzadeh suggested that the latter model fits the data significantly better.

The development of a fatigue performance model is dependent upon two factors. First, the representative performance lines for laboratory data must be correlated. Thus a shift factor should be developed to provide a compatible relationship between the laboratory and actual field observation. The model developed by Finn,et al. was based on a laboratory developed fatigue curve and in-situ pavement performance obtained from AASHO Road Test data. The Monismith laboratory fatigue model was modified and shifted to

account for crack progression in the asphalt layer. The shift factors were developed from field observations. The original laboratory fatigue model is as follows:

$$\log N_f = 14.82 - 3.291 \log (\epsilon/10^{-6}) - 0.854 \log (E/10^3).$$

Two fatigue relationships were developed. One to predict the number of load applications (N_f) up to 10 percent, and the other to predict (N_f) for 45 percent cracking or more in the wheel path area. The final distress prediction equations are as follow (Figure 10):

$$\log N_f (\leq 10\%) = 15.947 - 3.291 \log (\epsilon/10^{-6}) - 0.854 \log (E/10^3)$$

$$\log N_f (\geq 45\%) = 16.086 - 3.291 \log (\epsilon/10^{-6}) - 0.854 \log (E/10^3)$$

Since the Finn,et al. models were developed for conventional asphalt layer thickness (4-6 inches), Craus,et al. [44] used a similar procedure to derive fatigue models for thin asphalt concrete pavement. The new k_1 values for Craus,et al. models are 15.87 for 10 percent or less areal cracking in the wheel path and 15.988 for 30 percent or more. Craus,et al. chose the 30 percent crack level as criteria for the second model instead of 45 percent in the Finn,et al. models.

Elliott and Thompson [39] discussed a numerical analysis to establish appropriate values for the fatigue parameters (k_1 , k_2 , and k_3) based on the AASHO Road Test data. The resulting model is as follows:

$$\log N_f = 2.2340 - 3.16 \log \epsilon_{ac} - 1.4 \log E_{ac}$$

For thicker asphalt concrete pavement (pavements which have total asphalt concrete and granular base thickness of 15 inches or greater) the following model is recommended:

$$\log N_f = 2.4136 - 3.16 \log \epsilon_{ac} - 1.4 \log E_{ac}$$

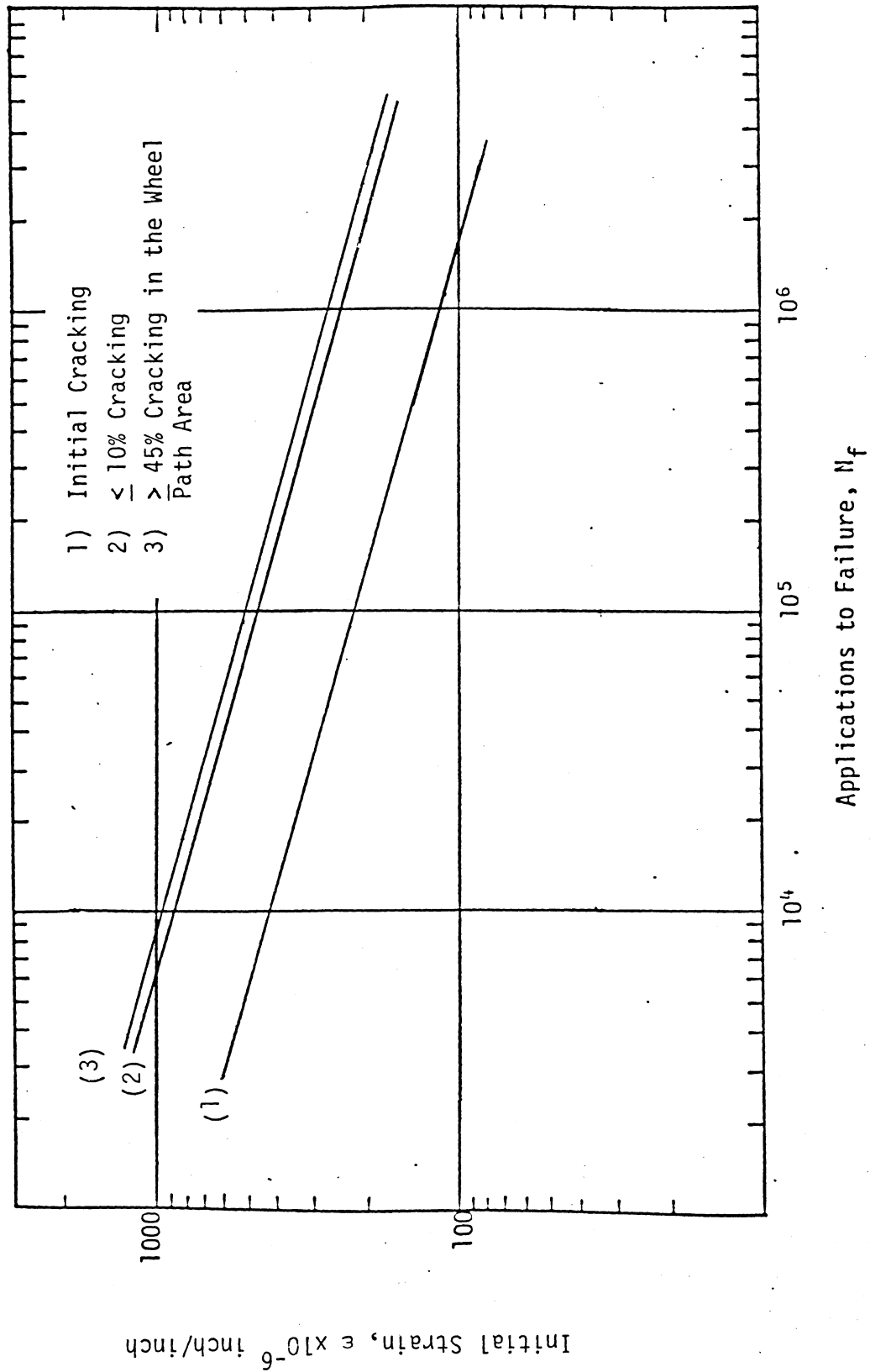


Figure 10. Relationship between Initial Cracking, 10% Cracking and 45% Cracking for Finn Fatigue Model.

where:

N_f = number of load applications until failure,

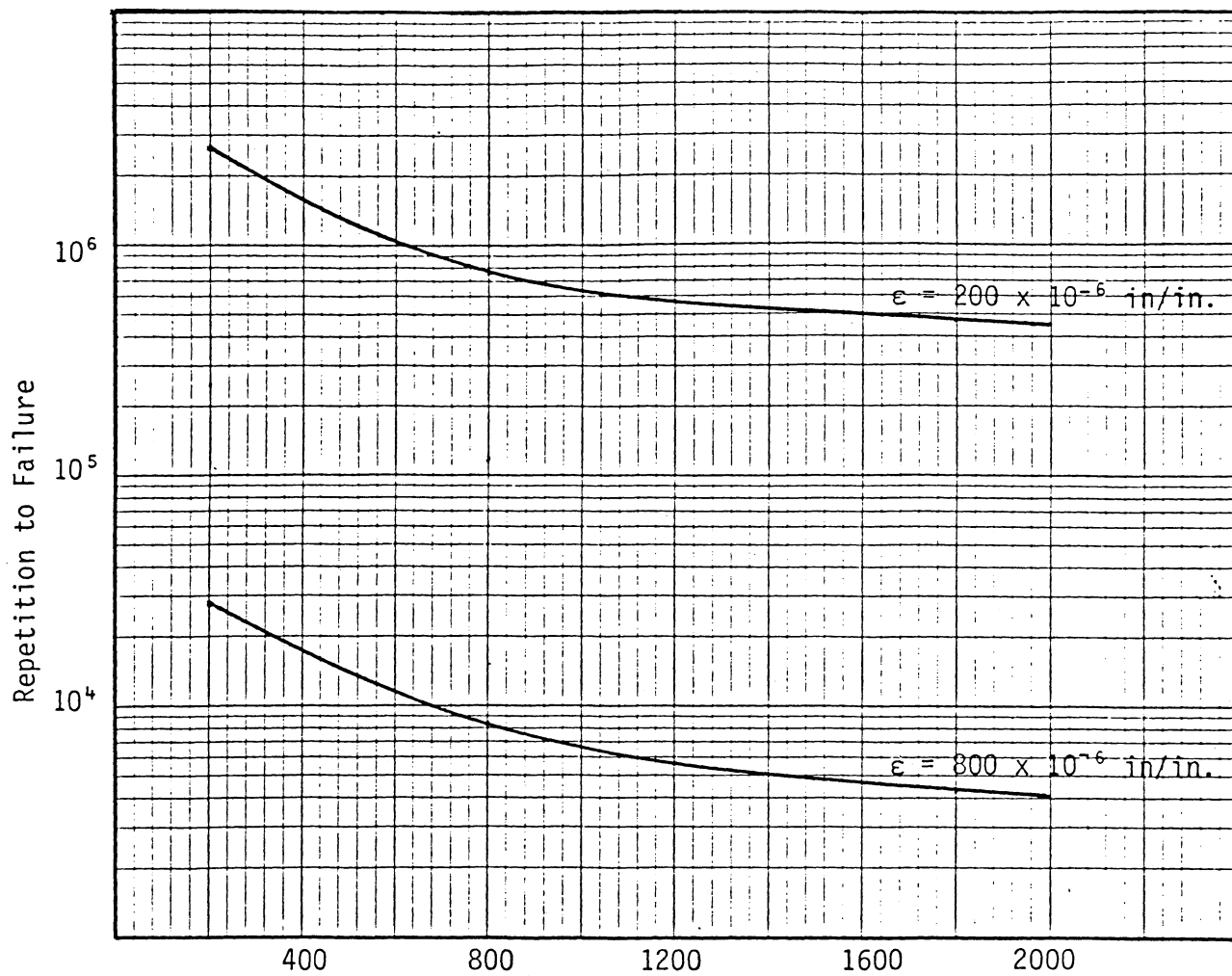
ϵ_{ac} = asphalt concrete tensile strain, in/in, and,

E_{ac} = asphalt concrete resilient modulus, psi.

Discussion

Due to the authors review of the literature and experience, it is currently felt that the Finn,etal. model is the most acceptable fatigue model. The same conclusion has been reached by Witczak and Bell when they evaluated the remaining life of the pavements using different fatigue models including Monismith model (recall that Finn,etal. fatigue model is based on Monismith Laboratory fatigue model). Witczak and Bell stated that " the most reasonable estimates of remaining life from elastic layered theory occurs with the use of Monismith fatigue criterion." [42]. Furthermore, this model allows for variations in mixture stiffness without excessive fluctuations in the position of the fatigue prediction curves as is the case with other models. The effect of stiffness fluctuation is more pronounced in the low to mid range of the stiffness value as shown in Figure 11. Table 4 is a numerical comparison between the models for a range of tensile strain.

Close examination of the Finn,etal. models indicates that pavement failure occurs in three stages. The first stage represents the life span of new pavement until the initial crack (generally a longitudinal crack). The second stage represents the life span between initial cracking until 10 percent cracking in the wheel path area. The third stage represents the life



Asphalt Concrete Modulus (ksi)

Figure 11. Effect of Stiffness Fluctuation
on Fatigue Life.

Table 4. Numerical Comparison Between Fatigue Models.

Researchers and References	Strain Levels		
	= 100 in/in	= 300 in/in	= 600 in/in
Pell and Brown [22, 23]	6.5×10^5	1.0×10^4	7.5×10^3
Monismith, et al. [24]	8.6×10^5	2.3×10^4	2.4×10^3
Kingham [25]	1.1×10^7	4.6×10^4	1.4×10^3
ARE [26]	4.4×10^6	1.5×10^4	4.2×10^3
Majidzadeh [30]	4.0×10^7	2.3×10^5	9.1×10^3
Finn, et al. [8] 10% cracking	1.1×10^7	3.1×10^5	3.2×10^4
Finn, et al. 45% cracking	1.6×10^7	4.3×10^5	4.3×10^4
Elliott and Thompson [39]	7.9×10^6	2.4×10^5	2.7×10^4
Elliot and Thompson [39] thick pavement (≥ 15 in)	1.2×10^7	3.7×10^5	4.1×10^4
Average	1.5×10^7	1.86×10^5	1.86×10^4

span between the 10 percent cracking until 45 percent cracking or more in the wheel path area (Figure 12). Assuming the second stage needs " N_f " traffic load repetitions to develop. The first stage needs $1/13 N_f$ and the third stage needs $1.38 N_f$ to develop. In essence, it only takes 38 percent more traffic loading for the cracking to progress from 10 percent to 45 percent or more. In the Finn,etal. models, two shift factors were used. A factor of 13 was used to adjust the number of traffic repetitions from initial cracking to 10 percent cracking and a factor of 18 for adjusting the number of traffic repetition from initial cracking to 45 percent cracking or more. If N_f represents the number of traffic repetition to 10 percent cracking in the wheel track, $1/13 N_f$ represents the number of load repetitions until the initial cracking. The ratio of the two factors $18/13$ (or 1.38) represents the additional traffic loading for the cracking to progress from 10 percent to 45 percent or more.

Another view of the Finn,etal. model is by the Damage Index (DI). Where DI is defined as unity in Miner's summation and the pavement is considered failed. Thus, a predicted DI of unity corresponds to 10 percent cracking and DI equal to 1.38 corresponds to 45 percent cracking. A representative curve line can be drawn through the two points as shown in Figure 13. Rauhut and Kennedy [27] have suggested the following equation be used in transforming predicted Damage Index to percentage of areal cracking (A_c):

$$A_c = 0.19 e^{3.96 DI}$$

Using this equation or Figure 13, the growth in areal cracking can be predicted for a given Damage Index or level of traffic based on the Finn,etal. model. Realizing the fact that the relation between crack progression and number of traffic repetitions is exponential to the fourth power (Rauhut and Kennedy equation) is critical to the design process. Most of the time

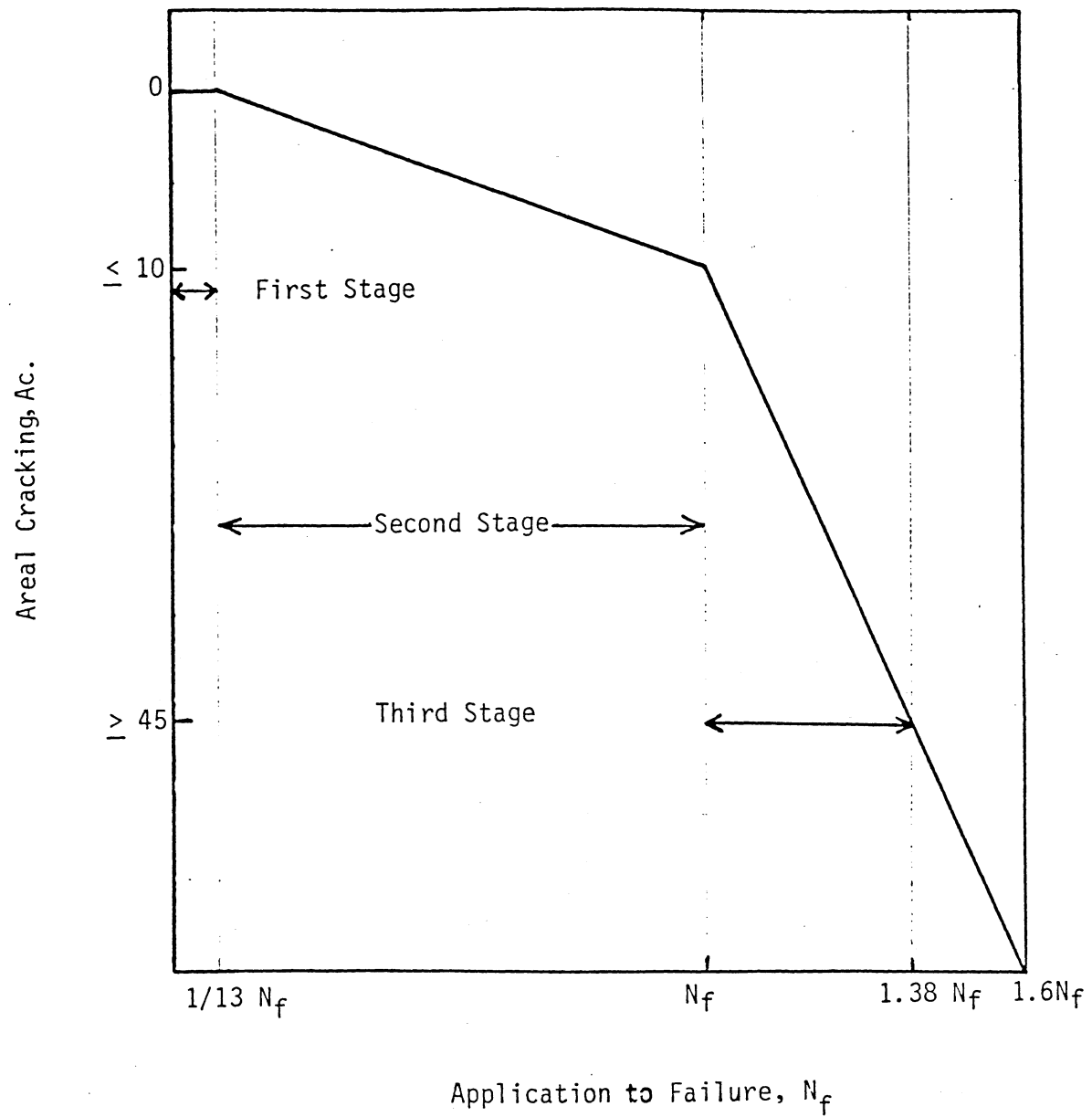


Figure 12. Pavement Life Cycle

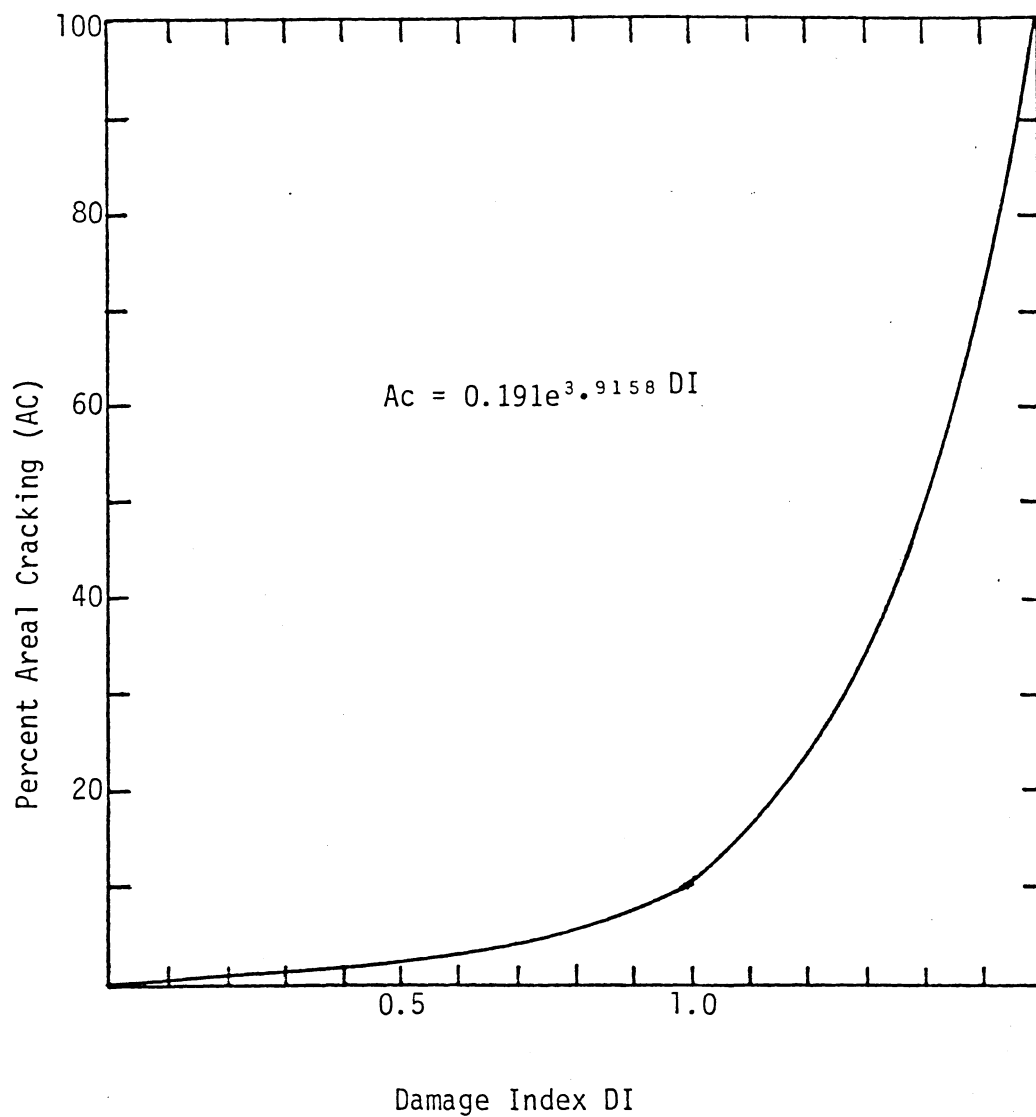


Figure 13. Relationship between Areal Cracking and Damage Index for Finn_{etal}. Fatigue Model (Ref. 27)

distressed pavement should be rehabilitated before the distress severity reaches 10 percent cracking. Once the distress level reaches this point the structural integrity of the pavement will deteriorate very rapidly.

An essential part of the "Development and Implementation of an overlay Design Study" is the definition of the relationship between pavement distress and performance in Washington State. The establishment of such relationship is considered a complex task. It is the consensus of researchers in pavement design that one of the largest deficiencies in pavement design systems is the absence of a reliable relationship of pavement performance to pavement distress.

Figure 14 demonstrates the complexity of relating distress to performance or the relationship between pavement rating and traffic (the assumption here is that pavement failure is based solely on fatigue). Figure 14 is a conceptual relationship that relates the pavement rating, percentage Areal Cracking, (A_c) Damage Index (DI), asphalt concrete tensile strain (ϵ_t) and number of traffic repetitions to failure (N_f). It is composed of two parts. The first part ties pavement rating based on fatigue with Areal Cracking (A_c) and Damage Index (DI). The second part consists of fatigue curves for initial, 10 percent and 45 percent or more cracking in the wheel track.

For a given fatigue pavement rating score, one can read the Damage Index and calculate the remaining life of the pavement. To find the number of load applications until failure, the Damage Index is projected to a prespecified strain level and extended to the fatigue line (either 10% or 45% cracking depending upon the distress level). There the number of load repetitions can be read.

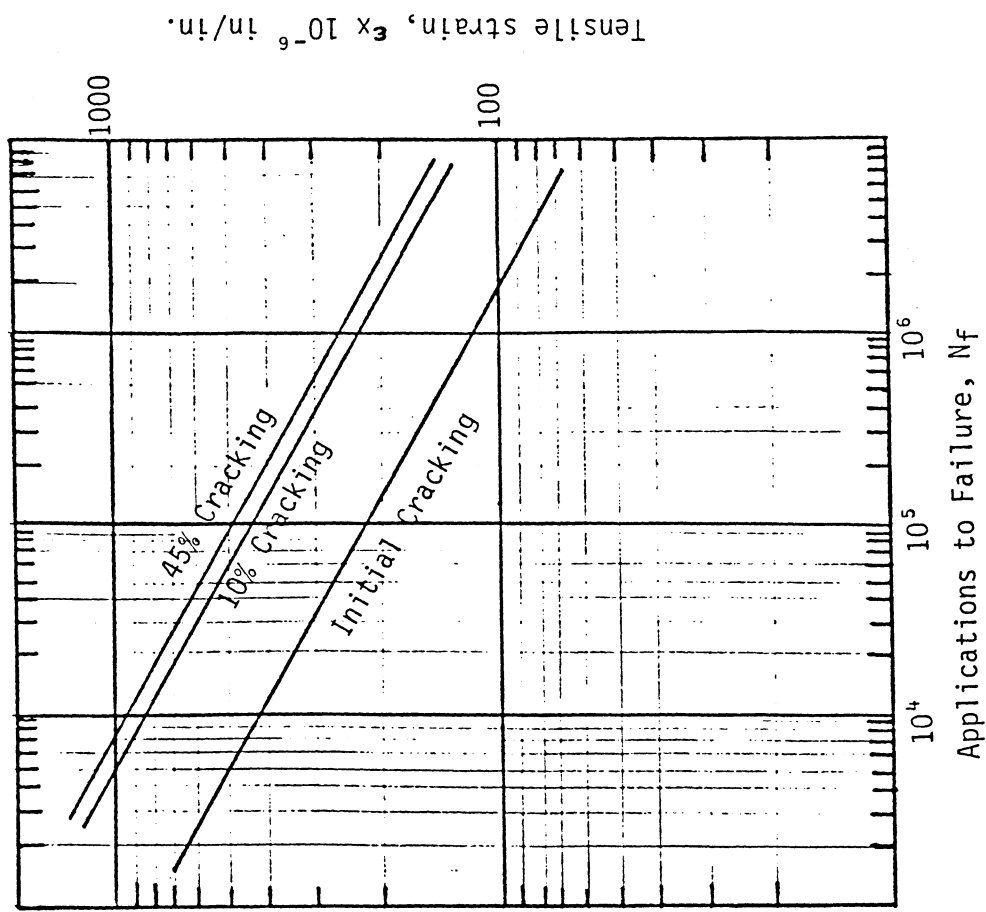
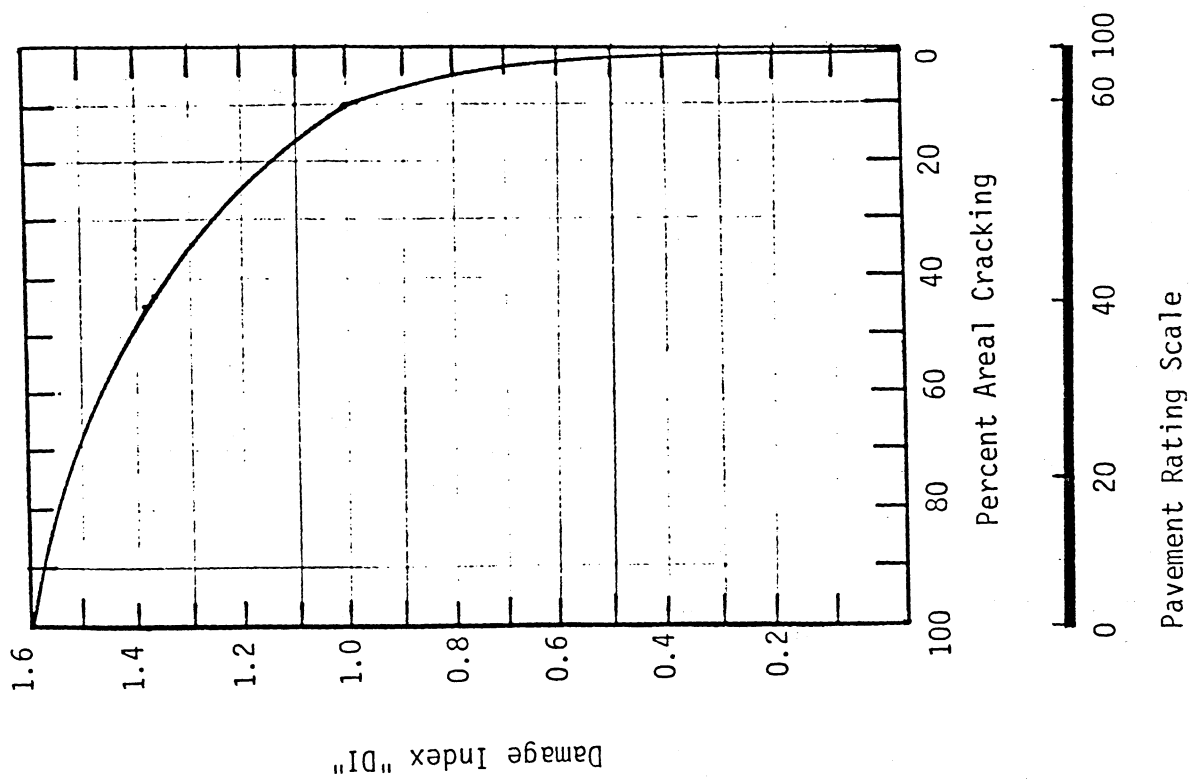


Figure 14. Nomographic Representation of Distress-Performance Relationship.

As mentioned before, Figure 14 represents the idea of relating distress to performance. Further studies are needed to refine this conceptual nomograph. Such a study includes:

1. a fatigue relationship for the State of Washington, and
2. the correlation between areal cracking and Damage Index.

Summary

The development of pavement performance models is dependent on two factors. First the representative performance lines for laboratory data must be correlated. Then consideration must be given to the need for a shift factor to provide a compatible relationship between the laboratory and actual field observations.

In this section, representative fatigue curves were discussed. The Finn,etal. model was selected as providing the most reliable estimate of asphalt concrete pavement life. This model expresses the fatigue life as a function of both the initial strain and the asphalt stiffness.

The relationship between distress and performance was also discussed briefly. The fact that it only needs a 38 percent increase in traffic load repetitions for the distress to progress from 10 percent cracking to more than 45 percent cracking in the wheel path places a strain on maintenance engineers.

REFERENCES

1. Terrel, R.L. and Rimsritong, S., "Pavement Response and Equivalencies for Various Truck Axle Tire Configuration," Research Report 17.1, Washington State Highway Commission, Olympia, Washington, 1974.
2. Mahoney, J.P., and Terrel, R.L., "Laboratory and Field Fatigue Characterization for Sulphur Extended Asphalt Paving Mixtures," Proceedings, Fifth International Conference on the Structural Design of Asphalt Pavements, 1982.
3. Lary, J.A., "LTM Site Models and a Comparison of Field and Laboratory Resilient Moduli," A report prepared for the Washington State Department of Transportation, Field Order No. F772559, Work Order No. 1-7327, December 1983.
4. Lary, J.A., Mahoney, J.P. and Sharma, J., "Evaluation of Frost Related Effects on Pavements," A report submitted to Washington State Department of Transportation, WSDOT Contract Y-2292, May 1984.
5. Terrel, R.L., and Krukar, M., "Evaluation of Test Tracking Pavements," Proceedings, Association of Asphalt Pavement Technologists, 1970.
6. McLeod, N.W., "Reduction in Transverse Pavement Cracking by Use of Softer Asphalt Cements," Control of Pavement Slipperiness-Asphalt Pavement Cracking, Special Report No. 101, Highway Research Board.
7. Heukelom, W., "A Bitumen Test Data Chart for Showing the Effect of Temperature on Mechanical Behavior of Asphaltic Bitumens," Journal of the Institute of Petroleum, November 1969.
8. Finn, F., Saraf, C., Kulkarni, R., Nair, K., Smith, W., and Abdullah, A., "The Use of Distress Prediction Subsystems for the Design of Pavement Structures," Proceedings, Fourth International Conference Structural Design of Asphalt Pavements, University of Michigan, 1977.

9. Asphalt Institute, Asphalt Overlays and Pavement Rehabilitation Manual, Series No. 17, College Park, MD, 1977.
10. Climatological Data, Washington State, 1983 and 1984.
11. Witczak, M.W., "Development of Regression Models for Asphalt Concrete Modulus for Use in MS-1 Study," Unpublished report, the Asphalt Institute, College Park, MD, 1978.
12. Hudson, W.R. and Kennedy, T.W., "An Indirect Tensile Test for Stabilized Materials," CFHR Research Report 98-1, Center for Highway Research, the University of Texas at Austin, January, 1968.
13. "Structural Design of Asphalt Concrete Pavements to Prevent Fatigue Cracking," Highway Research Board, Special report No. 140, Washington, D.C.
14. Hudson, W.R., Finn, F.N., Redigo, R.D., and Roberts, F.L., "Relating Pavement Distress to Serviceability and Performance," Federal Highway Administration, Report No. FHWA/RD-80/098, February 1981.
15. McLean, D.B. and Monismith, C.L., "Estimation of Permanent Deformation in Asphalt Concrete Layers Due to Repeated Traffic Loading," Proceedings, Association of Asphalt Paving Technologists, Vol. 43, 1974.
16. Monismith, C.L., "Rutting Prediction in Asphalt Concrete Pavements," A paper for the Symposium on Predicting Rutting in Asphalt Concrete Pavements, Transportation Research Board, Washington, D.C., January 1976.
17. McLeod, N.W., "Reduction in Transverse Pavement Cracking by Use of Softer Asphalt Cements," Control of Pavement Slipperiness-Asphalt Pavement Cracking, a Special Report No. 101, Highway Research Board, Washington, D.C., 1969.

18. Kasianchuk, D.A., Terrel, R.L., and Haas, R., "A Design System for Minimizing Fatigue, Permanent Deformation and Shrinkage Fracture Distress of Asphalt Pavements," Proceedings, Third International Conference on the Structural Design of Asphalt Pavements, 1972.
19. McDowell, C., "Pavement Cracking: Causes and some Preventive Measures," Control of Pavement Slipperiness-Asphalt Pavement Cracking, a Special Report No. 101, Highway Research Board, Washington, D.C., 1969.
20. Moore, R.M., "Development of Pay Adjustment System for Asphalt Concrete Pavements Using Layered Elastic Theory," Ph.D. Dissertation, University of Washington, 1981.
21. Adedimila, A.S., and Kennedy, T.W., "Fatigue and Resilient Characteristics of Asphalt Mixtures by Repeated-Load Indirect Tensile Test", Research Report 183-5, Center for Highway Research, The University of Texas at Austin, August 1975.
22. Pell, P.S. and Brown, S.F., "The Characteristics of Materials for the Design of Flexible Pavement Structures", Proceedings, Third International Conference on the Structural Design of Asphalt Pavements, September 1972.
23. Pell, P.S., "Characterization of Fatigue Behavior," Structural Design of Asphalt Concrete Pavements to Prevent Fatigue Cracking," Highway Research Special Report No. 140, Highway Research Board, Washington D.C., January 1973.
24. Monismith, C.L. and Epps, J.A., Asphalt Mixture Behavior in Repeated Flexure, Report No. TE-69-6, Institute of Transportation and Traffic Engineering, University of California, 1969.

25. Kingham, R.I., "Failure Criteria Developed from AASHTO Road Test Data," Proceedings, Third International Conference on the Structural Design of Asphalt Pavements, September 1972.
26. Austin Research Engineers, Inc., "Asphalt Concrete Overlays of Flexible Pavements," Vol. 1, Development of New Design Criteria, Report No. FHWA-RD-75-75, Federal Highway Administration, Washington, D.C., June 1975.
27. Rauhut, J.B., and Kennedy, T.W., "Characterizing Fatigue Life for Asphalt Concrete Pavements," Structural Performance of Pavement System, Transportation Research Board, Transportation Research Record No. 888, 1982.
28. Witczak, M.W., Pavement Performance Models, Volume 1: Repeated Load Fracture of Pavement Systems, U.S. Army Engineer, Waterways Experiment Station, Contract Report S-76-15, August 1976.
29. Nelson, T.L. and LeClerc, R.V., "Development and Implementation of Washington State's Pavement Management System," Washington State Department of Transportation, Report No. WA-RD 50.1, September 1982.
30. Majidadeh, K. and Ilves, G.J., "Flexible Pavement Overlay Design Procedures, Vol. 1: Evaluation and Modification of the Design Methods," Federal Highway Administration, Report No. FHWA/RD-81/032, August 1981.
31. Van der Poel, C., "A General System of Describing the Visco-Elastic Properties of Bitumens and Its Relation to Routine Test Data," Journal of Applied Chemistry, Vol. 4, 1954, P. 221.
32. Heukelom, W., "A Bitumen Test Data Chart for Showing the Effect of Temperature on the Mechanical Behavior of Asphaltic Bitumens," Journal of the Institute of Petroleum, November 1969.

33. Heukelom, W. and Klomp, A.J.G., "Road Design and Dynamic Loading," Proceedings, Association of Asphalt Paving Technologists, 1964.
34. Haas, R.C.G., "A Method of Design Asphalt Pavements to Minimize Low-Temperature Shrinkage Cracking," The Asphalt Institute, Research Report RR-73-1, College Park, Maryland, 1973.
35. Southgate, H.F., and Deeu, R.C., "Temperature Distribution Within Asphalt Pavements and Its Relationship to Pavement Deflection," Design, Evaluation and Performance of Pavement System, Highway Research Record No. 291, Washington, D.C., 1969.
36. Yoder, E., and Witczak, M., Principals of Pavement Design, John Wiley (1975).
37. Hwang, D. and Witczak, M.W., "Program Data (Chevron), User's Manual," University of Maryland, College Park, 1979.
38. Bonnaure, F., Gravois, A., and Udron, J., "A New Method for Predicting the Fatigue Life of Bituminous Mixes," Proceedings, the Association of Asphalt Paving Technologists, Vol. 49, 1980.
39. Elliott, R.P. and Thompson, M.R., "ILLI-PAVE Mechanistic Analysis of AASHO Road Test Flexible Pavement," A Paper submitted for the 1985 Annual Meeting of the Transportation Research Board (Draft), Washington D.C., January 1985.
40. Mahoney J.P., Terrel, R.L. and Cook, J.C., "Sulfur Extended Asphalt Pavement Evaluation in the State of Washington: SR 270 Highway Pavement Performance Report," A Report prepared for Washington State Transportation Commission, Department of Transportation, FHWA DOT-FH-11-9620, October 1982.
41. Mahoney, J.P., Tsuneta, J.Y., and Terrel, R.L., "Pavement Testing and Analysis of Heavy Hauls for SR 12," A Report prepared for Washington State

Department of Transportation, Olympia, Washington, Contract Agreement Y-144, Task No. 4, August 1979.

42. Witczak, M.W. and Bell, K.R., "Remaining Life Analysis of Flexible Pavements," Proceedings, Association of Asphalt Paving Technologists, Vol. 47, 1978.
43. Mahoney, J.P., Lary, J.A., Balgunaim, F., and Lee, T.C., "Sulfur Extended Asphalt Pavement Evaluation in the State of Washington: Laboratory Mixture Characterization," A report prepared for Washington State Transportation Commission, Department of Transportation, June 1982.
44. Craus, J., Yüce, R., and Monismith, C.L. "Fatigue Behavior of Thin Asphalt Concrete Layers in Flexible Pavement Structures, " A paper prepared for annual meeting of the Association of Asphalt Paving Technologists, 1984. (Draft Copy).

APPENDIX A

The Estimation of Stiffness Modulus of Bituminous

Materials by Shell Nomograph

Van der Poel [31] is usually acknowledged in the development of the first method to estimate asphalt stiffness. The penetration of asphalt at 77°F (ASTM D5) and the Ring-and-Ball softening point (ASTM D36) are needed for this procedure.

Heukelom [32] suggested that Van der Poel nomograph is not applicable for a number of North American asphalts such as blown asphalts and asphalts with high paraffin contents. Consequently, Heukelom developed a nomograph to be used in correcting the Ring-and-Ball temperature (R & B) with the Van der Poel nomograph.

McLeod [6] has also modified the Van der Poel nomograph. In this modification, McLeod developed another parameter that shows the temperature susceptibility of an asphalt in terms of Penetration Index (PI). This is referred to as the Penetration-Viscosity Number (PVN). The PVN is determined by values of penetration at 77°F and viscosity of 275°F. The relationship is defined by the equation:

$$PVN = \frac{\log L - \log X}{\log L - \log m} (-1.5)$$

where X = Viscosity of the asphalt under consideration at 275°F, centistokes,

L = Viscosity at 275°F for a PVN = 0.0 as determined from Figure A1,

and

m = Viscosity at 275°F for PVN = -1.5 as determined from Figure A1.

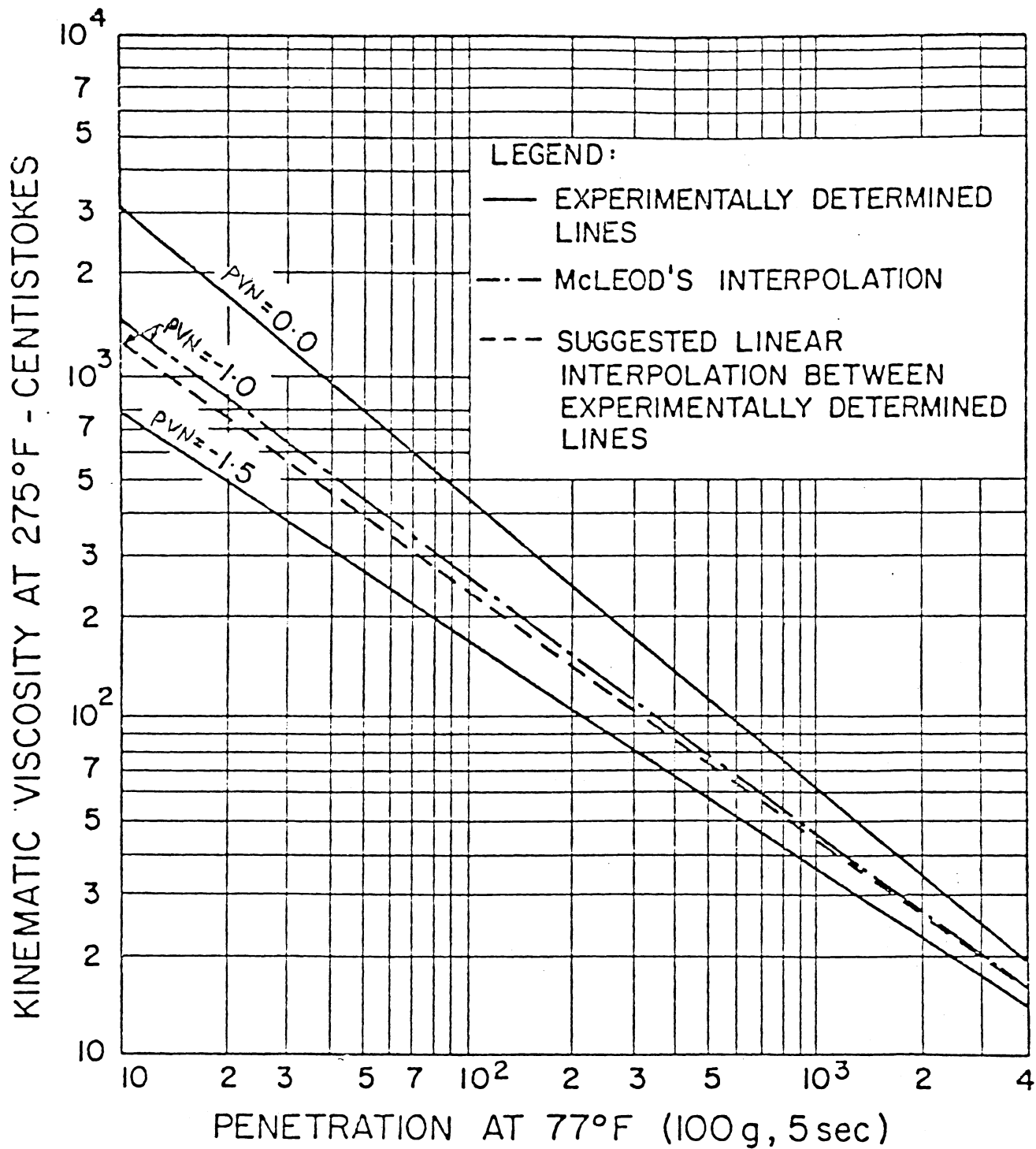


Figure A.1. McLeod's Chart for Estimating the P.I. (Ref. 17)

Next, the temperature difference is determined from Figure A2 (in this figure the Ring-and-Ball softening point is called "base temperature"). Then, the desired loading time is located on the bottom scale in Figure A3. This point is connected by a straight line to the temperature difference and penetration index scales. The asphalt stiffness is then read on the top curved logarithmic scale. A loading time of 0.1 sec. was used in this study.

In the LTM sties study, neither the Ring-and-Ball temperature nor the viscosity at 275°F was reported. The Ring-and-Ball temperature was estimated from the nomograph developed by Heukelom (Figure A4) and the viscosity at 275°F was estimated from the standard penetration-viscosity chart (Figure A5).

To estimate the stiffness of the mix, Heukelom and Klomp [33] have developed a formula which relates mix stiffness with stiffness of the binder. This formula is :

$$S_{mix}(t,T) = S_{bit}(t,T) \left[1 + \frac{2.5}{n} \times \frac{C_v}{1-C_v} \right]^n$$

where: S_{mix} = stiffness modulus of the mixture at a specific loading time

t , and temperature, T ,

S_{bit} = stiffness modulus fo binder,

$$n = 0.83 \log \frac{4 \times 10^5}{S_{bit}}$$

C_v = volume concentration of the aggregate,

$$\begin{aligned} &= \frac{\text{Volume of aggregate}}{\text{Volume of aggregate \& Volume of bitumen}} \\ &= \frac{100 - \% \text{ VMA}}{100 - \% \text{ Air}} \end{aligned}$$

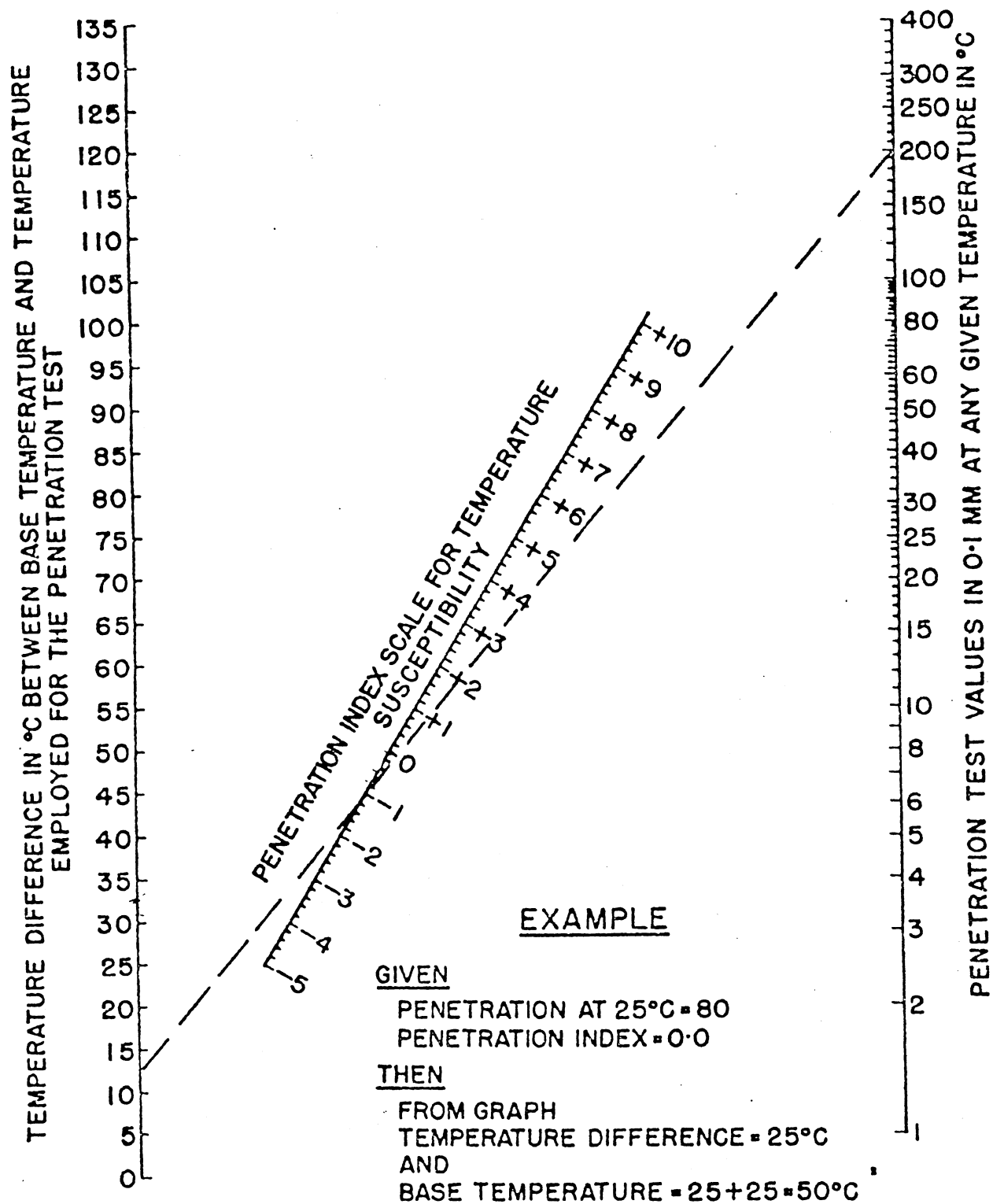


Figure A.2. Mcleod's Modification of Pfeiffer's and Van Doormal's Nomograph (Ref. 17)

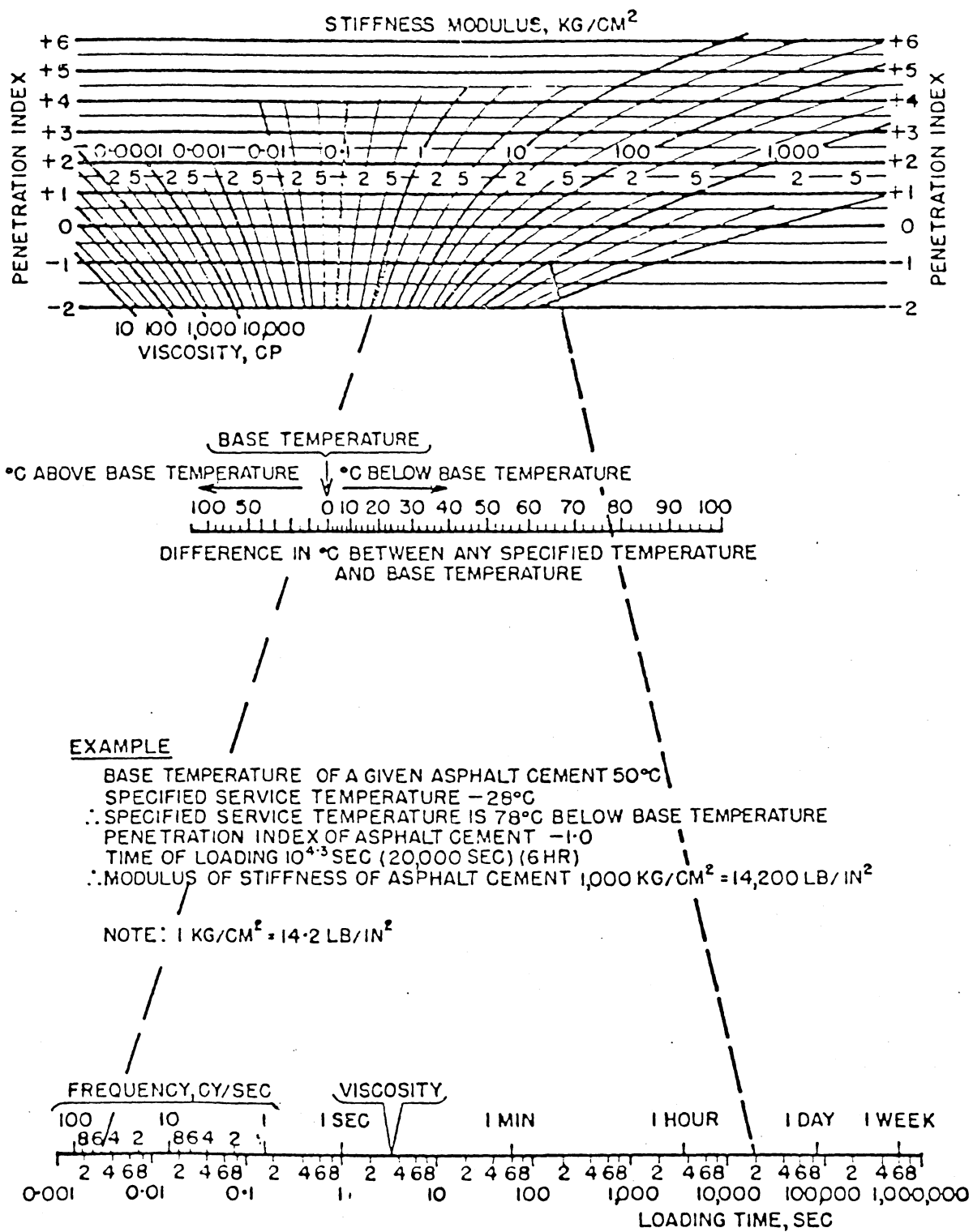


Figure A.3. McLeod's Modification to Van der Poel's Nomograph for Determining Asphalt Stiffness (Ref. 17)

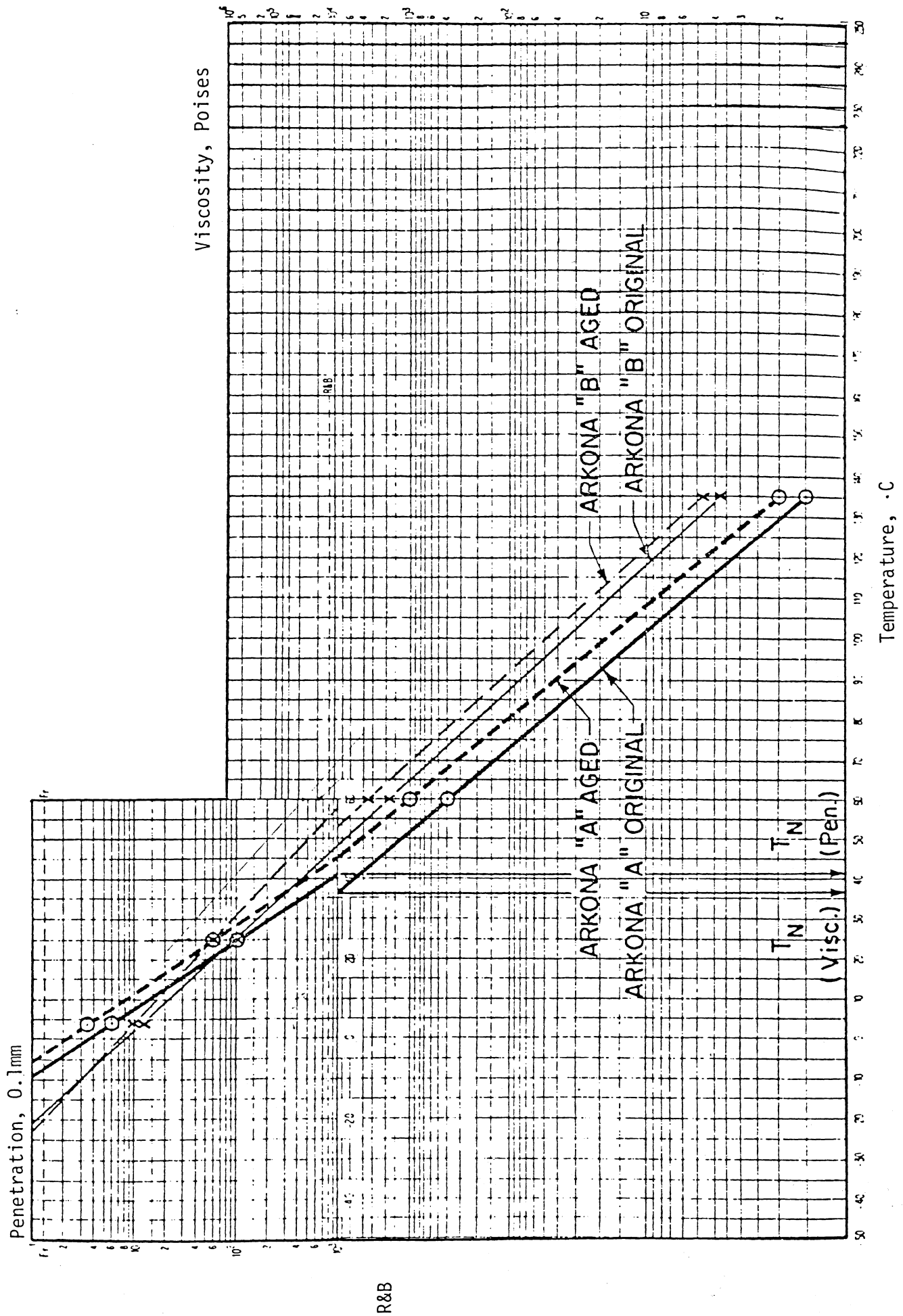


Figure A.4. Heukelom's Bitumen Test Data Chart (Ref. 34)

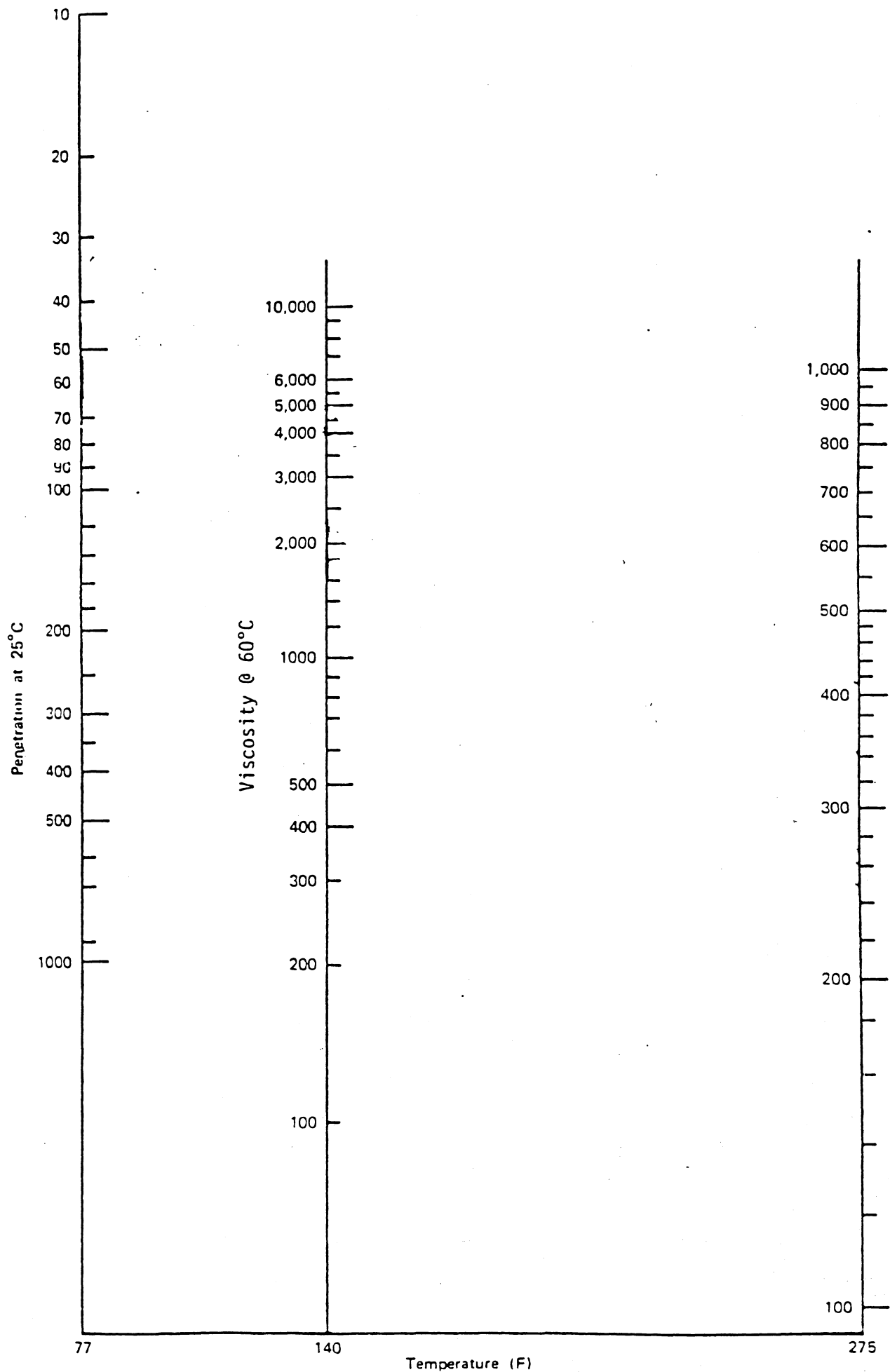


Figure A.5. Standard Penetration-Viscosity Chart

VMA = voids in mineral aggregate.

Figure A6 is a chart to solve this equation. The equation was developed for mixes with 3 percent air voids and C_v values between about 0.7 and 0.9. For mixes with air voids greater than 3 percent a corrected C_v' should be used.

$$C_v' = \frac{C_v}{1 + \Delta V}$$

where C_v' = corrected C_v value, and

$$\Delta V = (\text{actual \% air voids} - 3\%)/100$$

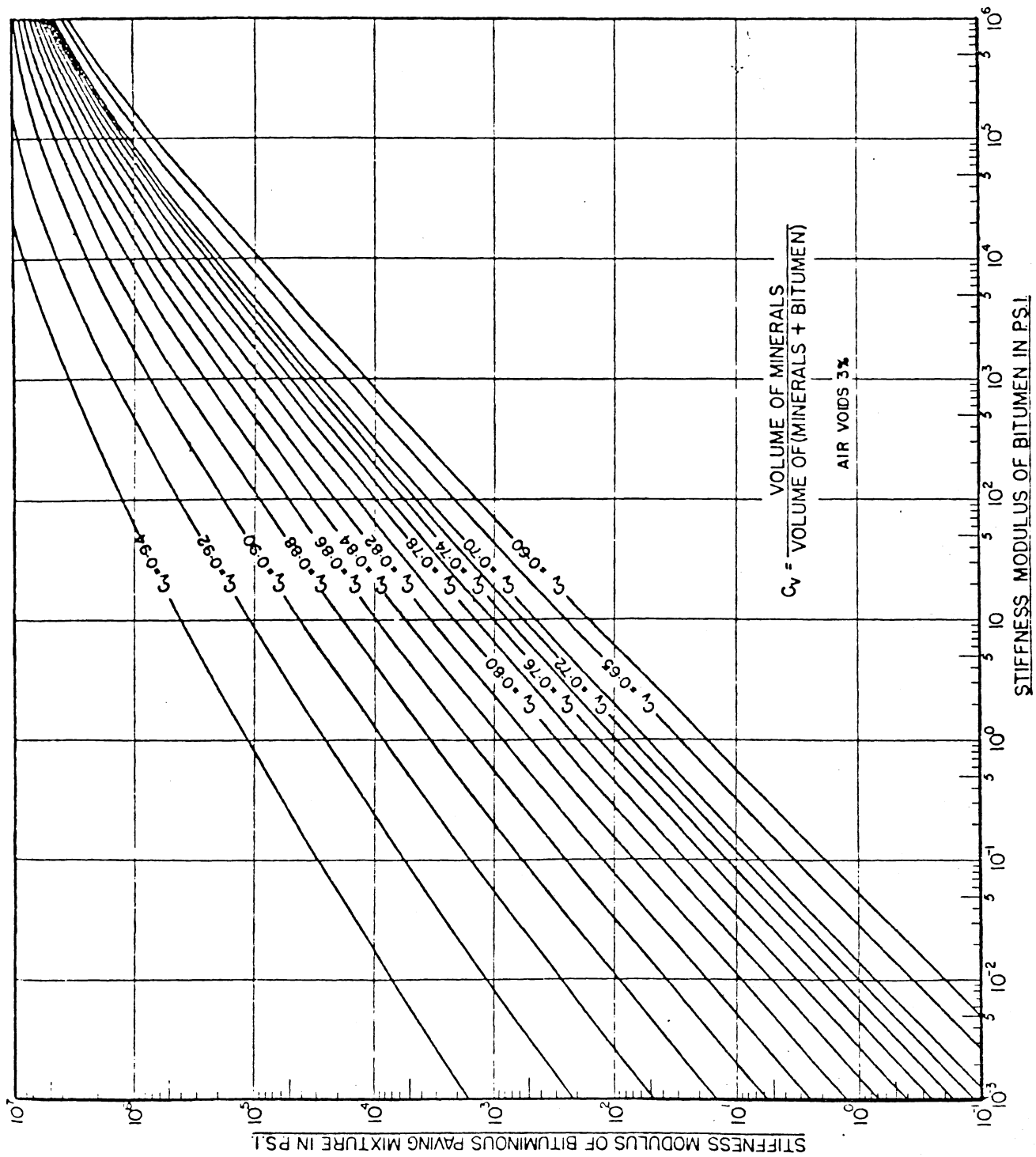


Figure A.6. Relationships Between Asphalt Cement Stiffness and Mix Stiffness
Based on Heukelom and Klomp Method. (Ref 34)

APPENDIX B

Methods for Predicting Mean

Pavement Temperature

Pavement temperature is an important factor in determining the in-situ resilient modulus of the asphalt layer. Pavement surface temperature might quantify some of the asphalt concrete temperature variation effects. On the other hand, temperature at depths are known to be a better indicator of these variations.

Based on the AASHO Road Test data, Southgate [35] developed a regression model that relates pavement surface temperature, air temperature history, and pavement temperature. Southgate suggested that "pavement temperature in the top 2 inches of the pavement are more directly dependent on the hour of the day and the amount of heat absorption, where temperatures at depths greater than 2 inches are assumed to be a function of the surface temperature, amount of heat absorption, and the past 5 days of temperature history." Consequently, Southgate developed sets of curves for each hour between 6 am and 5 pm. A condensed form of these curves is shown in Figure B1. Information needed for this method includes:

1. Maximum and minimum air temperature for each of the five days prior to the date of deflection testing. These can be obtained in one of the following methods [9]:
 - (a) By recording the hourly air temperatures for a period of five days preceding each test day,
 - (b) Temperature data can be obtained from the nearest weather station, or
 - (c) Temperature data can be obtained from published weather bureau data.

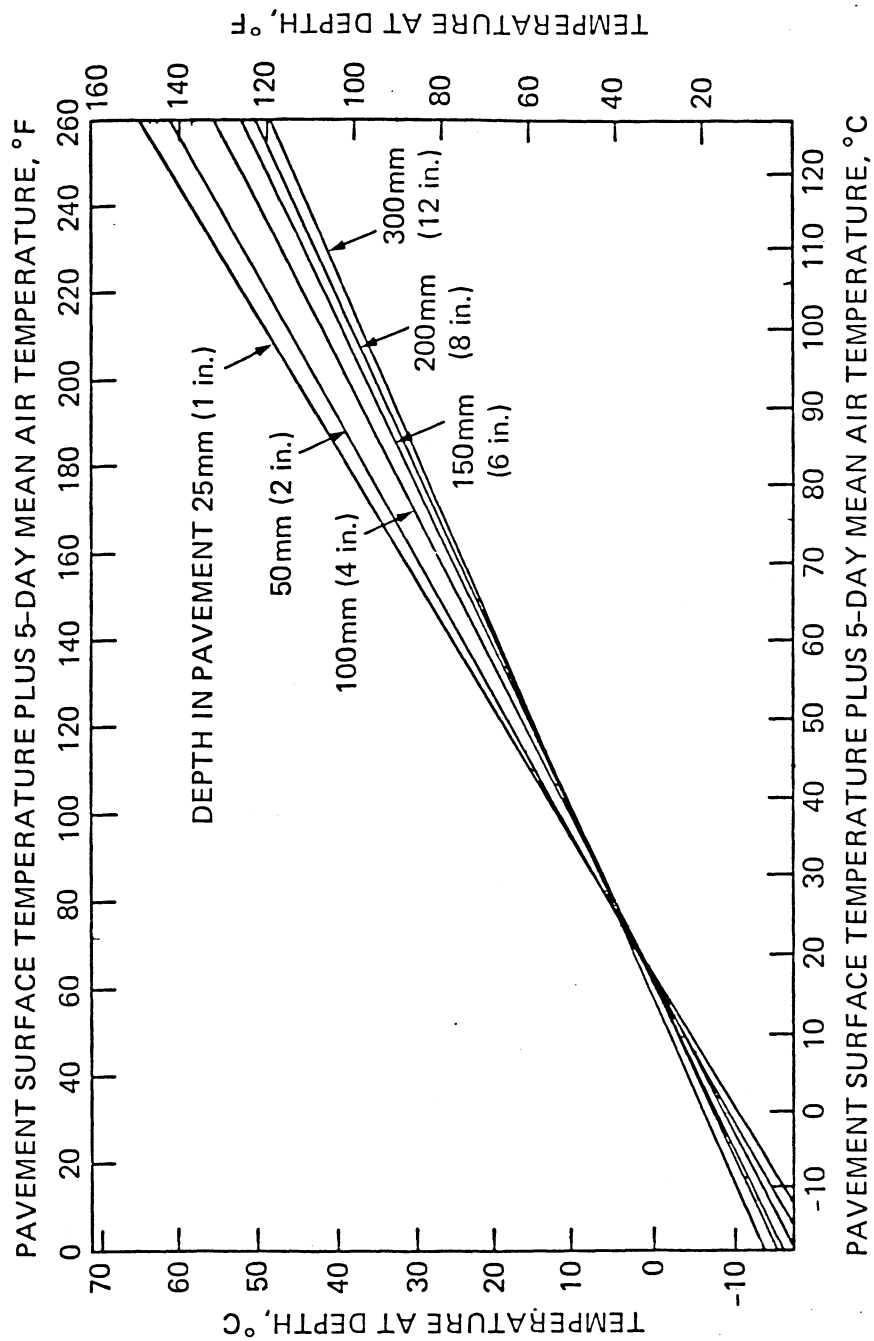


Figure B.1. Southgate's Chart for the prediction of Mean Pavement Temperature (Ref. 9).

The first step is to calculate the 5-day mean air temperature (average of maximum and minimum air temperatures for five days preceding the test), and add the result to the pavement surface temperature. Next, the temperature at any pavement depth can be read from Figure B.1. The mean pavement temperature equals the average of the surface temperature, the mid depth temperature and the bottom of asphalt layer temperature. The following example illustrates the procedure:

Pavement thickness = 6 in.

Surface temperature = 88 °F.

Average air temperature for 5 days preceding the test = 72 °F

Adjusted surface temperature = $88 + 72 = 160$ °F

Temperature at mid-depth (3 in), from Figure B.1 = 85 °F

Temperature at bottom (6 in), from Figure B.1 = 80 °F

Pavement mean temperature = $(72 + 85 + 80)/3 = 79$ °F

Another general method to estimate the pavement temperature was suggested by Witczak in Reference 36. This method estimates the average annual pavement temperature from the average annual air temperature by the following equation:

$$\text{MPT} = 1.05 \text{ MAT} + 5$$

where:

MPT = mean annual pavement temperature (F); and

MAT = mean annual air temperature (F).

Recently, Hwang and Witczak (37) suggested an empirical relationship to estimate the pavement temperature (surface and base layers).

This relation is:

Layer 1:

$$T_p = T_a \left(1 + \frac{3}{(h_1 + 12)} \right) - \frac{102}{h_1 + 12} + 6$$

Layer 2:

$$T_p = T_a \left(1 + \frac{3}{(3h_1 + h_2 + 12)} \right) - \frac{102}{3h_1 + h_2 + 12} + 6$$

where :

T_p = pavement temperature;

T_a = air temperature, and

h_1, h_2 = thickness of surface layer, base layer respectively.

Hwang and Witczak used this relation in the development of the DAMA Computer program.

APPENDIX C

Regression Analysis

Data from several pavement evaluation studies were pooled together for the regression analysis model. These studies are : the SR 270 highway pavement performance study, the SR 12 highway pavement study, the LTM sites study and the sulphur extended asphalt laboratory study.

The stiffness-temperature data is shown in Table C1. The first 15 data points represent the average values of the east and west bound of SR 27, the next 24 data points represent the mean values of resilient modulus test for SR 12 (each point is the average of five test points), the next 18 data points represent the mean values of the resilient modulus test for the LTM site (each point is the average of ten test points), and the last group of data points represent the mean values for the sulphur extended Asphalt Study.

To improve the normal distribution of the data, only the average values were considered rather than all available data. Table C.2 shows some statistical summary of the data.

Three regression models were examined, these models are:

$$\log Y = \beta_0 + \beta_1 X_1 + \epsilon_i \quad (1)$$

$$\log Y = \beta_0 + \beta_1 X_1^2 + \epsilon_i \quad (2)$$

$$\log Y = \beta_0 + \beta_1 X_1 + \beta_2 X_1^2 + \epsilon_i \quad (3)$$

where:

Y= Predicted resilient modulus,

X_1 = Temperature, °F

$\beta_0 \beta_1 \beta_2$ = regression parameters.

ϵ_i = error term

Comparing the three models, the second model gave the best fit according to the R-squared and the standard deviation. In all three models, three

Table C1. Stiffness- Temperature Data.

Count	Temp.	$M_R \times 10^3$	Count	Temp.	$M_R \times 10^3$
1	41.	1192.00	34	104.	89.40
2	41.	1570.00	35	104.	62.60
3	41.	1462.00	36	104.	95.70
4	41.	1267.00	37	104.	88.70
5	41.	1323.00	38	104.	91.50
6	77.	308.00	39	104.	67.80
7	77.	294.00	40	40.	2400.00
8	77.	447.00	41	40.	1910.00
9	77.	340.00	42	40.	2140.00
10	77.	292.00	43	40.	2710.00
11	104.	74.00	44	40.	2540.00
12	104.	81.00	45	40.	2130.00
13	104.	111.00	46	40.	2260.00
14	104.	62.00	47	40.	2810.00
15	104.	64.00	48	40.	2550.00
16	41.	1576.30	49	77.	541.00
17	41.	1452.00	50	77.	376.00
18	41.	1176.90	51	77.	464.00
19	41.	1449.00	52	77.	852.00
20	41.	1651.90	53	77.	477.00
21	41.	1348.60	54	77.	566.00
22	41.	1612.50	55	77.	546.00
23	41.	1335.60	56	77.	992.00
24	77.	417.70	57	77.	729.00
25	77.	383.00	58	41.	1216.00
26	77.	351.80	59	41.	1379.00
27	77.	175.50	60	41.	1384.00
28	77.	377.30	61	77.	249.00
29	77.	356.30	62	77.	238.00
30	77.	425.10	63	77.	246.00
31	77.	343.00	64	104.	46.00
32	104.	100.70	65	104.	56.00
33	104.	92.90	66	104.	56.00

points were identified as outliers. The final stiffness-temperature models is:

$$\log M_R = 6.47210 - 0.000147362 (T)^2$$

$$\text{or } M_R = 10[6.47210 - 0.000147362 (T)^2]$$

$$R\text{-square} = 93.4\%, \quad \text{Standard deviation} = 0.1394$$

where:

M_R = Asphalt Concrete resilient modulus, psi

T = Temperature, °F

The detailed regression model is shown in Figure C1. In addition the 90 and 95 percent prediction interval for a range of pavement temperature were calculated. The prediction intervals were calculated by the following equation:

$$y \pm t_{\alpha/2\sigma} \left[1 + \frac{1}{n} + \frac{(X_p - \bar{X})^2}{S_{xx}} \right]^{1/2}$$

Where y = predicted temperature, °F

$t_{\alpha/2}$ = the t-test value based on (n-2) degrees of freedom,

σ = standard error,

n = number of test points,

X_p = Predicted temperature,

\bar{X} = average temperature, and

$$S_{xx} = \sum (X_i - \bar{X})^2$$

The same regression model can be rewritten using the natural logarithmic form as:

$$M_R = \text{EXP} [14.9026 - 0.0003391(T)^2]$$

where M_R and T as defined before.

Table C.2. A Statistical Summary of the
Stiffness-Temperature Data.

Temperature °F	Number of Points	Maximum $M_R \times 10^3$	Minimum $M_R \times 10^3$	Average $M_R \times 10^3$	Standard Deviation
40	9	2810.0	1910.0	2308.3	297
41	16	1651.9	1177.0	1402.2	149
77	25	992	175.5	432.5	193
104	16	111.0	48.0	77.6	18.7

THE REGRESSION EQUATION IS
 $Y = 6.47 - .0001 X_1$

	COLUMN	COEFFICIENT	ST. DEV. OF COEF.	T-RATIO = COEF/S.D.
--		6.47210	0.03168	204.33
X1	SQ-TEMP	-0.000147362	0.000004847	-30.40

THE ST. DEV. OF Y ABOUT REGRESSION LINE IS
 $S = 0.1394$
 WITH (66- 2) = 64 DEGREES OF FREEDOM

R-SQUARED = 93.5 PERCENT
 R-SQUARED = 93.4 PERCENT, ADJUSTED FOR D.F.

ANALYSIS OF VARIANCE

DUE TO	DF	SS	MS=SS/DF
REGRESSION	1	17.95874	17.95874
RESIDUAL	64	1.24336	0.01943
TOTAL	65	19.20210	

Figure C1. The Regression Analysis for the Stiffness-Temperature Data.

